

# L-Type Amino Acid Transporter 1 Enables the Efficient Brain Delivery of Small-Sized Prodrug across the Blood–Brain Barrier and into Human and Mouse Brain Parenchymal Cells

Ahmed B. Montaser,\* Juulia Järvinen, Susanne Löffler, Johanna Huttunen, Seppo Auriola, Marko Lehtonen, Aaro Jalkanen, and Kristiina M. Huttunen

Cite This: <https://dx.doi.org/10.1021/acscemneuro.0c00564>

Read Online

ACCESS |

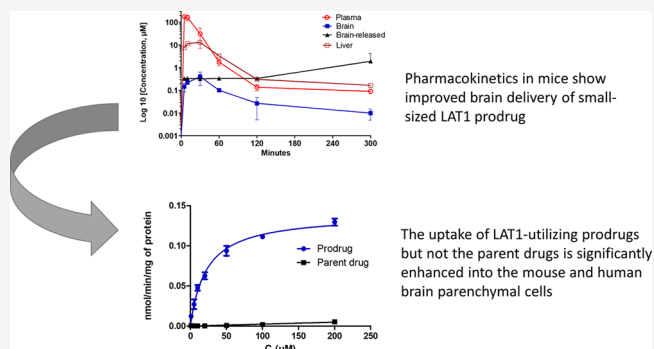
Metrics & More

Article Recommendations

Supporting Information

**ABSTRACT:** Membrane transporters have long been utilized to improve the oral, hepatic, and renal (re)absorption. In the brain, however, the transporter-mediated drug delivery has not yet been fully achieved due to the complexity of the blood–brain barrier (BBB). Because L-type amino acid transporter 1 (LAT1) is a good candidate to improve the brain delivery, we developed here four novel LAT1-utilizing prodrugs of four nonsteroidal anti-inflammatory drugs. As a result, all the prodrugs were able to cross the BBB and localize into the brain cells. The brain uptake of salicylic acid (SA) was improved five times, not only across the mouse BBB but also into the cultured mouse and human brain cells. The naproxen prodrug was also transported efficiently into the mouse brain achieving less peripheral exposure, but the brain release of naproxen from the prodrug was not improved. Contrarily, the high plasma protein binding of the flurbiprofen prodrug and the premature bioconversion of the ibuprofen prodrug in the mouse blood hindered the efficient brain delivery. Thus, the structure of the parent drug affects the successful brain delivery of the LAT1-utilizing prodrugs, and the small-sized LAT1-utilizing prodrug of SA constituted a successful model to specifically deliver its parent drug across the mouse BBB and into the cultured mouse and human brain cells.

**KEYWORDS:** L-type amino acid transporter 1 (LAT1), LAT1-utilizing prodrugs, intracellular brain drug delivery, transporter-mediated brain delivery, BBB, pharmacokinetics



## 1. INTRODUCTION

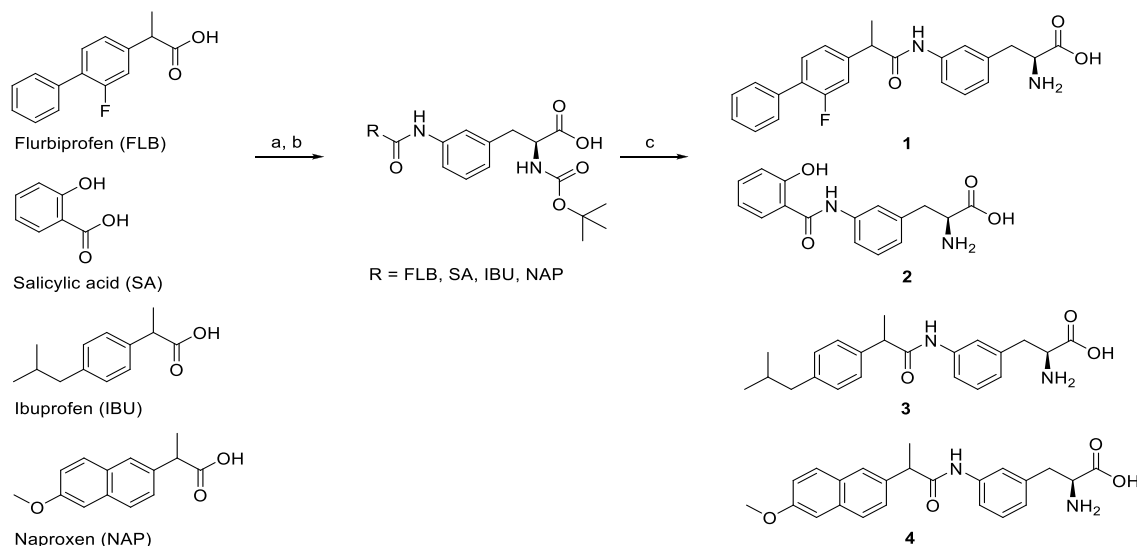
Membrane transporters are integral transmembrane proteins expressed ubiquitously on the cellular or blood–organ interfaces in order to control the permeability of solutes and nutrients.<sup>1</sup> In the blood–brain barrier (BBB), for instance, the transporters have been estimated to constitute 10–15% of all proteins in the neurovascular unit.<sup>2</sup> Hence, transporters have been utilized as drug targets to develop outstanding therapies. For example, inhibition of glucose and sodium transporters led to the development of clinically approved antidiabetic and diuretic drugs, respectively, such as gliflozins and thiazides.<sup>3</sup> Moreover, influx transporters regulate the drug dispositions, and thus, they are considered potential drug carriers. For example, the drug delivery of some oral antiviral drugs, such as valacyclovir and valganciclovir, has been improved via utilizing intestinal transporters.<sup>4,5</sup>

Transporters expressed at the BBB have been investigated as effective drug carriers into the brain. It has been found, for instance, that the dopamine prodrug (levodopa), baclofen, melphalan, gabapentin,<sup>6</sup> and pregabalin<sup>7</sup> utilize L-type amino

acid transporter 1 (LAT1) to reach their target sites in the brain. Therefore, LAT1 utilization is generally considered very promising regarding the effective brain delivery. Among over 20 carriers expressed on the BBB, LAT1 showed better characteristics over the other amino acid, glucose, organic cation/anion, choline, or monocarboxylic acid transporters.<sup>8</sup> Despite the low transport capacity of LAT1 compared to that of glucose transporter(s),<sup>9</sup> LAT1 is highly and selectively expressed in both luminal and abluminal sides of the BBB.<sup>10,11</sup> In addition, LAT1 is also expressed in mouse brain parenchymal cells such as astrocytes and microglia.<sup>12</sup> Moreover, LAT1 utilization does not interrupt the brain amino acid homeostasis,<sup>8,13,14</sup> and its expression and function are not altered by the

Received: August 28, 2020

Accepted: November 6, 2020

Scheme 1. Synthetic Steps for the Preparation of Prodrugs 1–4<sup>a</sup>

<sup>a</sup>Reagents and conditions: (a)  $\text{SOCl}_2$ ,  $\text{CH}_2\text{Cl}_2$ , reflux, overnight; (b) BOC-L-3-aminophenylalanine, NaOH,  $\text{CH}_2\text{Cl}_2$ , RT, overnight, 44–88%; (c) TFA,  $\text{CH}_2\text{Cl}_2$ , RT, overnight, 51–74%.

Table 1. Physicochemical Properties and Protein Binding of the Studied Compounds

compound	molecular weight (Mw) (g/mol)	cLogD <sub>pH 7.4</sub>	unbound drug fraction ( $f_w$ , %) ( $n = 3$ , mean $\pm$ SD)		
			mouse serum	mouse liver S9	mouse brain S9
prodrug 1	406.46	2.22	1.07 $\pm$ 0.31	0.84 $\pm$ 0.32	1.17 $\pm$ 0.30
FLB	244.27	1.41	0.97 $\pm$ 0.16	11.09 $\pm$ 1.19	38.00 $\pm$ 1.83
prodrug 2	300.31	−0.43	81.69 $\pm$ 7.94	60.59 $\pm$ 15.59	50.62 $\pm$ 16.63
SA	138.12	−1.47	0.71 $\pm$ 0.03	46.17 $\pm$ 9.21	51.44 $\pm$ 3.70
prodrug 3	368.48	2.12	17.80 $\pm$ 4.80	15.07 $\pm$ 4.22	5.75 $\pm$ 0.03
IBU	206.29	1.71	0.09 $\pm$ 0.05	18.74 $\pm$ 2.89	34.09 $\pm$ 6.01
prodrug 4	392.46	1.26	13.63 $\pm$ 1.03	1.97 $\pm$ 0.20	5.86 $\pm$ 2.17
NAP	230.26	0.25	0.12 $\pm$ 0.01	41.06 $\pm$ 8.61	64.65 $\pm$ 2.75

inflammatory insult.<sup>15</sup> Therefore, LAT1 is believed to transport its substrates across the BBB and the cellular barriers of the brain parenchyma effectively and harmlessly.

LAT1 is a nonglycosylated membrane protein and commonly referred and shortened from a heterodimeric complex of LAT1 light chain and 4F2hc (CD98) heavy chain.<sup>16</sup> The transport activity of LAT1 is dependent on both heterodimeric subunits but independent of the surrounding media such as pH or sodium. LAT1 exchanges large and neutral amino acids such as L-leucine (L-Leu), L-histidine, and L-phenylalanine (L-Phe) as well as thyroid hormones across the plasma membranes. Since LAT1 has been first cloned<sup>16</sup> several studies have investigated the structural features for optimal LAT1 utilization.<sup>17–19</sup> Hence, a prodrug approach has emerged that suggests the conjugation of the parent drugs to natural LAT1 substrates such as L-Phe or L-tryptophan.<sup>19–25</sup> As a consequence, LAT1-utilizing prodrugs of ketoprofen, ferulic acid, dopamine, and valproic acid were developed based on the published quantitative structure–activity relationship (QSAR) model.<sup>19</sup> The *in vitro* cellular uptake, *in situ* rat brain perfusion, and pharmacokinetics studies of the previously mentioned prodrugs have paved the way to identify the best amino acid moiety and conjugation site for optimal LAT1 utilization. However, it is still unclear whether the structures of the parent drug play a role in the brain uptake and the intracellular localization in brain cells following the LAT1 prodrug approach. Therefore, and in light of these latest

findings, we developed four novel LAT1-utilizing prodrugs of four nonsteroidal anti-inflammatory drugs (NSAIDs) by conjugation to the same amino acid moiety. We investigated the brain and liver distribution *in vivo* and the intracellular uptake of these prodrugs into cultured human and mouse brain parenchymal cells with the aim to improve the brain delivery and the intracellular localization of the anti-inflammatory drugs.

Neuroinflammation is a hallmark of the neurodegenerative diseases.<sup>26</sup> Thus, our main goal is to deliver the anti-inflammatory drugs specifically into the brain and further target them into the activated astrocytes and microglia, which are releasing most of the inflammatory mediators<sup>27,28</sup> in the brain. Consequently, neuroinflammation can be alleviated, and hence, better therapies can be developed for neurodegenerative diseases.

## 2. RESULTS

**2.1. Drug Design.** Our research group has previously reported five LAT1-utilizing prodrugs of ketoprofen having structurally different promoieties in their prodrug structure.<sup>20</sup> According to these results and in accordance to our previously published 3D-QSAR model,<sup>19</sup> the phenylalanine attached at the meta position of the aromatic ring with an amide bond to the parent drug has the highest ability to utilize LAT1 for cellular and brain uptake after intraperitoneal administration to mice. Therefore, in the present study, this L-Phe-promoiety was

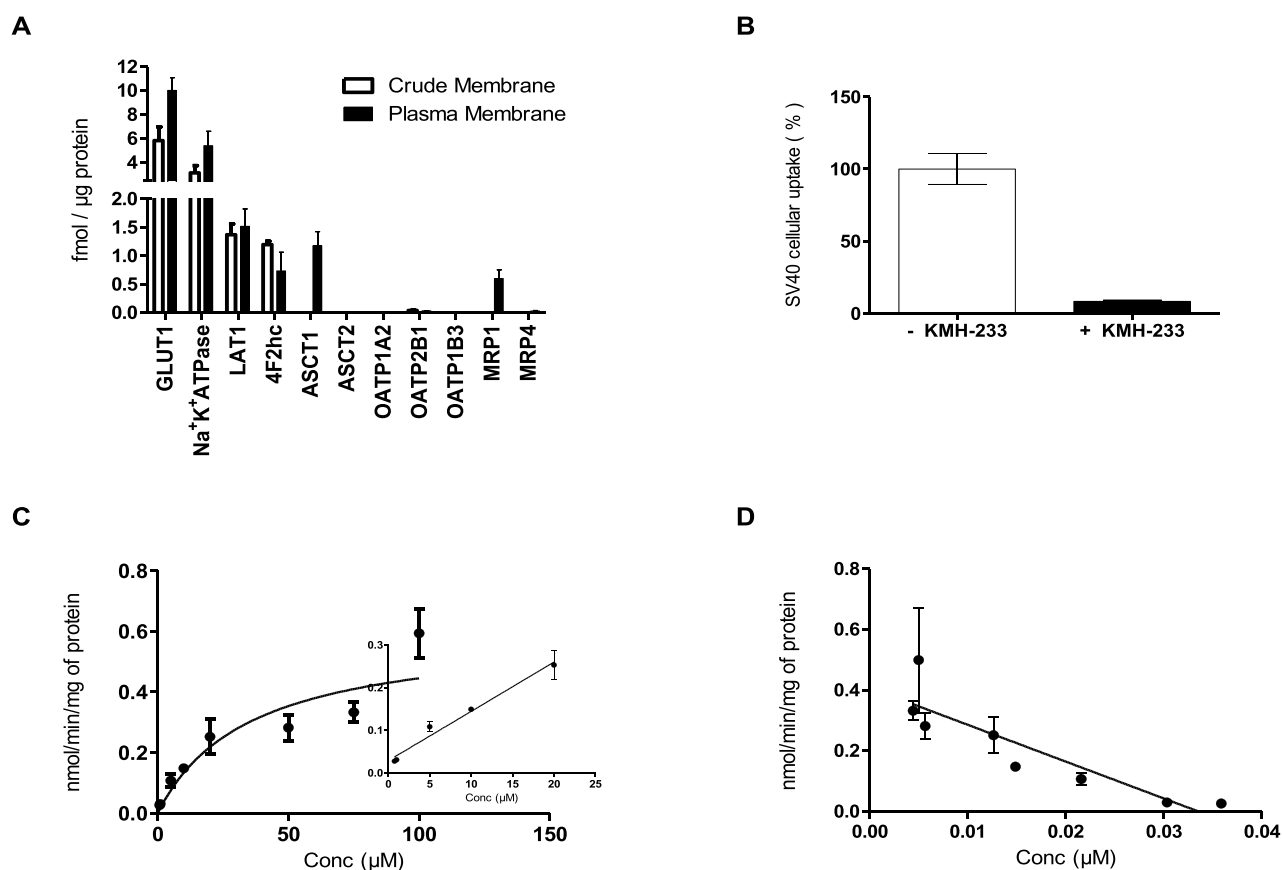


**Figure 1.** Membrane transport in SV40 cells is demonstrated by (1) the protein expression levels of LAT1, 4F2hc, GLUT1, Na<sup>+</sup>K<sup>+</sup>ATPase, ASCT1, OATP1A2, OATP2B1, OATP1A2, OATP2B1, OATP1B3, MRP1, and MRP4 in the crude membrane (□) and plasma membrane (■) fractions. The results are presented as mean ± SD ( $n = 3$ ).

derivatized by a similar manner with four different anti-inflammatory drugs, namely, flurbiprofen (FLB), salicylic acid (SA), ibuprofen (IBU), and naproxen (NAP). The amide bond was selected to produce prodrugs that are stable enough in the mouse first-pass metabolism enabling the highest possible brain drug delivery without premature bioconversion. We have previously reported that this is impossible to achieve in mice with, e.g., ester prodrugs.<sup>23,29,30</sup> Other alternatives would have been to produce prodrugs with carbamate or carbonate bonds; however, due to the acid group of the selected parent drugs, only amide or ester prodrugs are possible to be designed. The prodrugs 1–4 were synthesized as previously described<sup>21</sup> with overall good yields after two steps (Scheme 1). Briefly, FLB, SA, IBU, or NAP was converted to corresponding acid chlorides by refluxing the acids with thionyl chloride. The acid chlorides were then coupled with *tert*-butyloxycarbonyl (BOC)-protected 3-aminophenylalanine, prepared as previously described,<sup>21</sup> in the presence of sodium hydroxide. The intermediates were finally deprotected by trifluoroacetic acid to give desired prodrugs 1–4.

**2.2. Pharmaceutical Properties of the Studied Compounds.** The physicochemical properties of the prodrugs and their nonspecific protein binding were studied and compared to those of their parent drugs (Table 1). The calculated distribution coefficients ( $c\text{Log}D_{\text{pH } 7.4}$ ) of all the prodrugs ( $2 < 4 < 3 < 1$ ) were higher than those of their corresponding parent drugs. Furthermore,  $c\text{Log}D$  values correlated significantly with the unbound fractions of the prodrugs ( $Y = -18.07 \pm 4.2 c\text{Log}D + 39.20 \pm 6.9$ ,  $R^2 = 0.9059$ ) in brain homogenates (supplementary data, Figure S1). For instance, the least

lipophilic prodrug (prodrug 2,  $c\text{Log}D = -0.43$ ) showed the highest percentage of unbound portions in mouse plasma ( $81.69 \pm 7.94$ ), brain S9 ( $50.62 \pm 16.63$ ), and liver S9 ( $60.59 \pm 15.59$ ) fractions. In contrast, the highest lipophilic prodrug (prodrug 1,  $c\text{Log}D = 2.22$ ) showed the lowest percentage of unbound portions in mouse plasma ( $1.07 \pm 0.31$ ), brain S9 ( $1.17 \pm 0.30$ ), and liver S9 ( $0.84 \pm 0.32$ ) fractions.

**2.3. Chemical and Enzymatic Stability of the Studied Prodrugs.** The stability and bioconversion of the prodrugs were followed over a period of 6 h in mouse and human plasma as well as in liver and brain S9 subcellular fractions. The amounts of the prodrugs and the released parent drugs were quantified after incubation in different conditions at several time points by liquid chromatography–tandem mass spectrometric methods (LC–MS/MS) as described in Liquid Chromatography–Tandem Mass Spectrometry Analysis section. Prodrugs 2–4 were completely stable in all the conditions (supplementary data, Table S1). However, prodrug 1 was completely stable only in mouse and human plasma but exhibited about 30% degradation in mouse and human S9 liver fractions as well as in mouse brain after 6 h incubation. Because the degradation percentage was almost the same among all media, it is likely that the degradation was chemical and not enzymatic.

**2.4. Membrane Transporters in the Immortalized Human Microglia.** A functional LAT1 transporter was identified earlier in the primary mouse astrocytes and BV2 cells.<sup>12</sup> Here, we evaluated the expression of LAT1/4F2hc transporter as well as some common influx and efflux transporters such as ASCT1, ASCT2, OATP1A2, OATP2B1,

OATP1B3, MRP1, and MRP4 in the human immortalized microglia (SV40) using the LC–MS/MS method described in the *Membrane Transporters in the Immortalized Human Microglia* section. The amounts of LAT1 light subunit ( $1.37 \pm 0.19$  fmol/ $\mu$ g protein) and 4F2hc heavy subunit ( $1.19 \pm 0.06$  fmol/ $\mu$ g protein) in the crude membrane fraction of SV40 cells were almost equal (Figure 1A). In the plasma membrane fraction, however, the amount of LAT1 ( $1.52 \pm 0.3$  fmol/ $\mu$ g protein) was slightly higher than 4F2hc ( $0.73 \pm 0.34$  fmol/ $\mu$ g protein). Other influx transporters such as ASCT1 and efflux transporter such as MRP1 were markedly expressed (Figure 1A), whereas the expressions of ASCT2, OATP1A2, OATP2B1, OATP1B3, and MRP4 were low or under the detection limits. Additionally, both membrane transporters GLUT1 and Na<sup>+</sup>/K<sup>+</sup>ATPase, which were used as markers of consistent cellular fractionation,<sup>31</sup> were detected in good yield and low variation between the replicates.

Moreover, we evaluated the function of LAT1 in SV40 cells via a concentration-dependent uptake study using [<sup>14</sup>C]-L-Leu as a probe substrate (Figure 1 B–D) and in the presence and absence of a selective LAT1 inhibitor (KMH-233).<sup>24</sup> The LAT1 inhibitor was able to inhibit the uptake of [<sup>14</sup>C]-L-Leu significantly ( $92 \pm 0.72\%$  inhibition) (Figure 1B). In addition, the uptake of [<sup>14</sup>C]-L-Leu was linear over the range  $0.76$ – $20$   $\mu$ M and was saturated at higher concentrations ( $>100$   $\mu$ M) with a  $V_{\max}$  value of  $530$  pmol/(min  $\times$  mg protein) and  $K_m$  value of  $26.7$  (Figure 1C). Moreover, the Eadie-Hofstee plot did not show any other transport system for [<sup>14</sup>C]-L-Leu in SV40 cells (Figure 1D).

**2.5. Lat1 Utilization in the Cultured Brain Cells.** The cellular kinetics of the parent and their prodrugs were evaluated against the functional LAT1 transporter in the primary mouse astrocytes, BV2 and SV40 cells. The binding affinity and transport capacity were evaluated by the ligand-competition uptake and total cellular uptake studies, respectively. As expected, the parent drugs were not able to inhibit the uptake of [<sup>14</sup>C]-L-Leu in any of the studied cell types. In contrast, all the prodrugs inhibited the uptake of [<sup>14</sup>C]-L-Leu with  $IC_{50}$  values in the low micromolar range ( $0.4$ – $54$   $\mu$ M; Table 2). While

**Table 2.**  $IC_{50}$  values of L-Leucine inhibition by the prodrugs

compound	$IC_{50}$ ( $\mu$ M) of L-Leucine uptake		
	astrocyte	BV2	SV40 cell
prodrug 1	$2.88 \pm 1.46$	$6.00 \pm 1.47$	$0.43 \pm 1.45$
prodrug 2	$21.30 \pm 1.24$	$18.88 \pm 1.62$	$21.10 \pm 1.33$
prodrug 3	$17.66 \pm 1.17$	$13.02 \pm 1.21$	$54.17 \pm 1.33$
prodrug 4	$7.66 \pm 1.13$	$10.16 \pm 1.14$	$16.88 \pm 1.88$

prodrug 1 was the most potent to utilize LAT1, the other prodrugs showed similar and consistent potencies in all the cell types. Moreover, the selective LAT1 inhibitor (KMH-233) significantly reduced the uptake of prodrug 2 ( $25$ ,  $50$ , and  $100$   $\mu$ M) and prodrug 1 ( $50$  and  $100$   $\mu$ M) in all the cell types (Figure 2). In contrast, the uptake of prodrugs 3 and 4 was not affected by the LAT1 inhibitor, and that was consistent in all the cell types.

**2.5.1. LAT1 Transport Capacity.** The total cellular uptake is another kinetic parameter that directly explains the transport capacity in the cultured cells. After 30 min incubation with the cells, the uptake of the studied compounds was measured by LC–MS/MS. Interestingly, the prodrugs but not the parent drugs were transported efficiently into all the cell types

(supplementary data, Figures S2, S3, and S4). Additionally, the Eadie-Hofstee plot revealed that the prodrugs were able to utilize a secondary transport system at the higher concentrations (supplementary data, Figures S5, S6, and S7). This was particularly seen for prodrugs 1, 3, and 4 in SV40 cells as compared to the other cell types (Table 3). However, prodrug 2 showed a consistent uptake pattern in all the cell types. Moreover, prodrugs 3 and 4 showed significantly lower transport capacity as compared to those of the other prodrugs in astrocytes ( $V_{\max} = 2.6$  and  $0.4$  pmol/(min  $\times$  mg protein), respectively) and in BV2 cells ( $V_{\max} = 9.6$  and  $3$  pmol/(min  $\times$  mg protein), respectively).

Furthermore, all the prodrugs were able to utilize LAT1 in higher affinity ( $K_m = 1.7$ – $20.8$   $\mu$ M) values than those of L-Leu ( $K_m = 26.7$ – $85.8$   $\mu$ M) in all the cell types (Table 4).

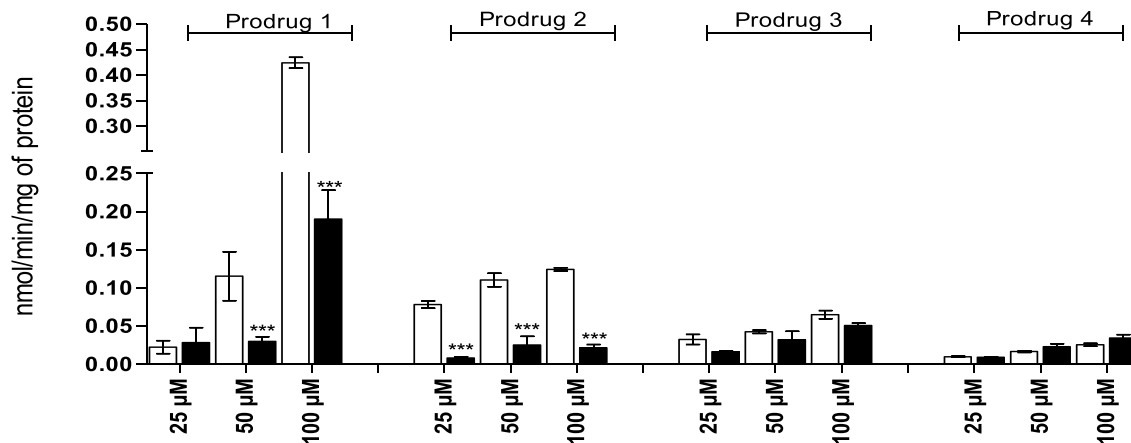
**2.6. Pharmacokinetic Study in Mice.** As the prodrugs showed promising in vitro cellular uptake, this encouraged us to examine their in vivo pharmacokinetics in mice. After administrating a bolus intraperitoneal (i.p.) injection of  $25$   $\mu$ mol/kg to the mice, we followed the drug's concentrations in the plasma, brain, and liver over a period of 5 h. All prodrugs and their parent drugs were rapidly absorbed to the systemic circulation. They reached the peak concentration in plasma ( $C_{\max}$  plasma =  $55$ – $205$  nmol/mL) already  $5$ – $10$  min after drug administration (Table 4). Importantly, all prodrugs rapidly penetrated the brain (within  $2$ – $30$  min after drug administration) with peak concentrations varying between  $0.2$  and  $1.2$  nmol/g brain (Figure 3 and Table 4). At each time point, the drug concentration ratio  $C_{\text{brain}}/C_{\text{plasma}}$  was higher for prodrugs 1, 2, and 4 than that of their parent drugs (Figure 4) indicating improved plasma-to-brain distribution. Except for prodrug 3, which showed slow brain distribution, and its  $C_{\text{brain}}/C_{\text{plasma}}$  ratios remained lower than those of the parent drug IBU for up to 120 min.

Moreover, to better understand the distribution kinetics between plasma and different organs, we calculated the distribution coefficients for brain and liver ( $K_p$  and  $K_{p,u}$  values) in respect to the total or the unbound concentrations in plasma, respectively (Table 4). In the case of total brain exposure and regardless of the plasma protein binding, the AUC ratios between the brain and plasma varied between  $0.003$  and  $0.03$  among prodrugs (Table 4). Notably, prodrugs 1 and 4 showed higher  $K_p$  values ( $0.02$  and  $0.03$ ) than those of their corresponding parent drugs ( $0.006$ ) indicating higher total brain exposure. In contrast, prodrug 2 showed a slightly lower  $K_p$  value as compared to that of SA, while prodrug 3 showed a considerably lower  $K_p$  value as compared to that of IBU. However, because the  $K_p$  value overlooks the differences in plasma protein binding, it is crucial also to calculate the  $K_{p,u}$  values. Prodrug 1 had a substantially higher  $K_{p,u}$  value ( $2.7$  fold) than that of its parent drug FLB, indicating improved BBB penetration, because a higher fraction of the unbound prodrug 1 in plasma had distributed into the brain. Contrarily, prodrugs 2, 3, and 4 had lower  $K_{p,u}$  values than those of their parent drugs.

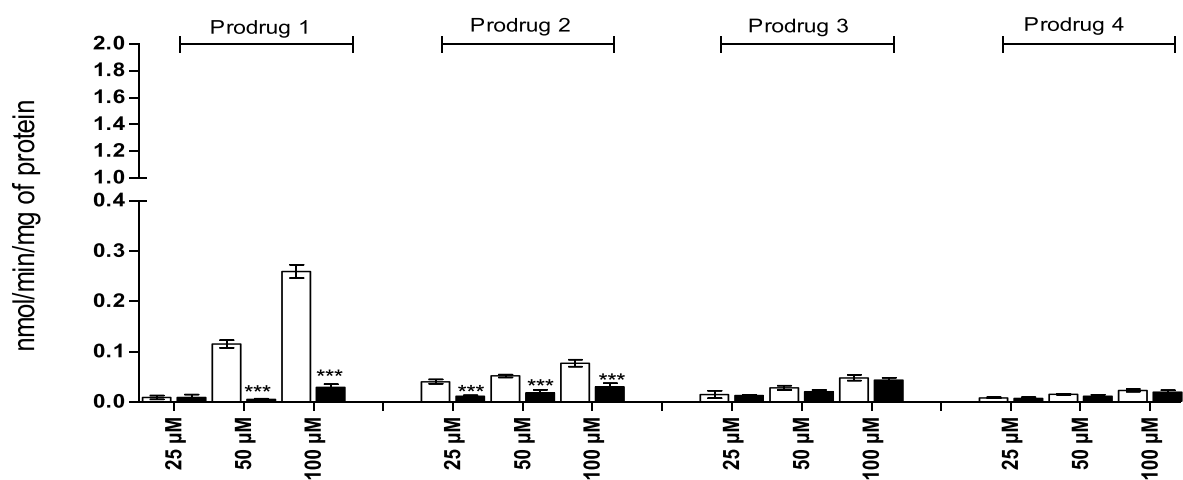
However, the improved brain delivery of the prodrug across the BBB does not merely guarantee improved efficacy, because the prodrug still needs to release the parent drug in the brain. Importantly, prodrug 2 released its parent drug SA specifically and considerably in the mouse brain, as indicated by a 5-fold higher  $K_{p,u}$  value than that of SA itself.

Similarly, prodrug 4 was able to release NAP in mouse brain but to a lesser extent than prodrug 2, as indicated by nearly half

A



B



C

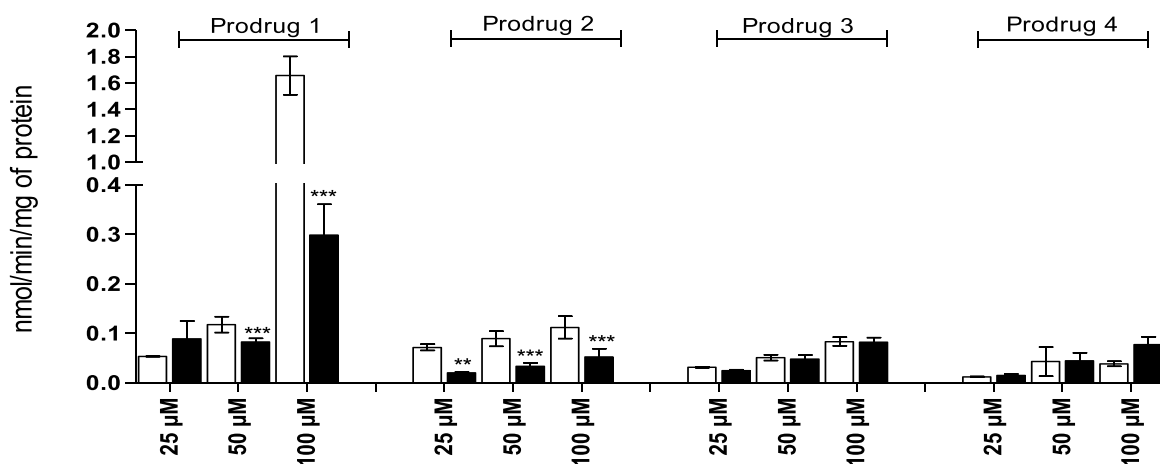


**Figure 2.** Cellular uptake of the prodrugs in the presence (■) and absence (□) of the selective LAT1 inhibitor (KMH-233) in mouse astrocytes (A), BV2 cells (B), and SV40 cells (C). The results are expressed as mean  $\pm$  SD ( $n = 3$ ) and analyzed by one-way ANOVA followed by Bonferroni's multiple comparison test; asterisks denote statistical significance \*\*\*  $P < 0.0001$ .

$K_{p,u\_brain}$  value as compared to that of NAP itself. In contrast, prodrugs 1 and 3 did not release their parent drugs in the mouse

brain. Interestingly, the parent drugs were not detected in the mouse liver after the prodrugs' administration over the period of

Table 3. Kinetics of prodrugs cellular uptake

	transport system	$V_{\max}$ (pmol/(min $\times$ mg protein))			$K_m$ ( $\mu$ M)		
		astrocyte	BV2	SV40	astrocyte	BV2	SV40
prodrug 1	LAT1	42.3 $\pm$ 13.0	26.3 $\pm$ 6.0	234.2 $\pm$ 0.0	3.2 $\pm$ 3.0	2.0 $\pm$ 1.0	4.8 $\pm$ 1.0
	other(s)	432.4 $\pm$ 100.0	NI <sup>a</sup>	3133.0 $\pm$ 1.0	262.5 $\pm$ 23.0	NI	306.7 $\pm$ 42.0
prodrug 2	LAT1	44.5 $\pm$ 5.0	27.3 $\pm$ 2.0	39.4 $\pm$ 0.0	4.5 $\pm$ 1.0	3.5 $\pm$ 0.0	2.2 $\pm$ 1.0
	other(s)	134.4 $\pm$ 16.0	108.3 $\pm$ 5.0	134.8 $\pm$ 5.0	39.3 $\pm$ 14.0	47.2 $\pm$ 5.0	19.8 $\pm$ 2.0
prodrug 3	LAT1	2.6 $\pm$ 0.0	9.6 $\pm$ 1.0	75.2 $\pm$ 0.0	1.7 $\pm$ 0.0	2.9	3.4 $\pm$ 1.0
	other(s)	42.6 $\pm$ 6.0	55.1 $\pm$ 9.0	NI	232.5 $\pm$ 8.0	117.5 $\pm$ 29.0	NI
prodrug 4	LAT1	0.4 $\pm$ 0.0	3.0 $\pm$ 1.0	13.0 $\pm$ 3.0	1.7 $\pm$ 1.0	20.8 $\pm$ 7.0	4.3 $\pm$ 2.0
	other(s)	7.3 $\pm$ 0.0	NI	NI	209.0 $\pm$ 38.0	NI	NI
[ <sup>14</sup> C]-L-Leu	LAT1	2920.0 $\pm$ 400.0 <sup>b</sup>	840.0 $\pm$ 100.0 <sup>b</sup>	530.0 $\pm$ 40.0	65.9 $\pm$ 14.0 <sup>b</sup>	85.8 $\pm$ 19.0 <sup>b</sup>	26.7 $\pm$ 6.0

<sup>a</sup>NI = not identified due to insufficient data. <sup>b</sup>Published elsewhere.<sup>12</sup>

5 h. At the same time, prodrugs 1, 2, and 4 released small amounts of their corresponding parent drugs (3, 0.7, and 4%, respectively) in the mouse plasma, while prodrug 3 already released 26% of its parent drug IBU in the mouse plasma.

### 3. DISCUSSION

Neuroinflammation and the brain delivery of therapeutical agents are important issues to consider in order to combat the neurodegenerative diseases. Epidemiological studies have shown contradictory results about using the NSAIDs in preventing some neurodegenerative diseases, and the clinical trials have failed to reach their efficacy end points.<sup>32,33</sup> These failures may be due to the difficulties in selecting the target population, dosing, and duration of NSAID exposure. Furthermore, the significant peripheral side effects of NSAIDs may restrict their long-term use. Nonetheless, there is a strong therapeutic rationale for the use of NSAIDs in restoring the dysregulation of glial cells characteristic of the neurodegenerative processes. For instance, they can modulate several inflammatory mediators such as cyclooxygenases,  $\gamma$ -secretases, and NF- $\kappa$ B.<sup>34</sup> Immunomodulation such as the inhibition of the voltage-gated K<sup>+</sup> channel Kv1.3 can also reduce the microglia activation and the associated inflammatory responses.<sup>35</sup> Thus, the improved delivery of NSAIDs or immunomodulatory drugs across the BBB and specifically into the activated microglia and astrocytes could also improve their pharmacological outcomes in neurodegenerative diseases.

Transporter-mediated brain delivery via a prodrug approach constitutes a promising way to deliver drugs into the brain.<sup>36</sup> The improved brain delivery of the LAT1-utilizing prodrugs is evident and reported in several studies.<sup>19–25</sup> However, the released amount of the parent drugs from the amide prodrugs in the mouse or rat brain has been too low. However, the balance between efficient brain uptake and sufficient release of the amide and ester prodrugs vs their premature bioconversion in plasma is very delicate. Moreover, the species differences in prodrug activating enzymes among rodents and humans makes the translation challenging. Therefore, we, for example, study amide and ester prodrugs in parallel, as it is highly likely that ester prodrugs can be suitable prodrugs in human situation. In the present study, we examined whether the structural differences of four NSAIDs contribute to the brain delivery of the LAT1-utilizing amide prodrugs and the release of the parent drugs into the mouse brain. In addition, the findings from this study can also be applied to the other neuroprotective and immunomodulatory drugs.

**3.1. Prodrug's Synthesis, Physicochemical Properties, and Protein Binding.** We selected structurally different NSAIDs such as FLB, SA, IBU, and NAP due to the differences in their lipophilicities ( $c\text{Log}D_{\text{pH } 7.4} = -1.47\text{--}2.2$ , Table 1) and molecular weights (138–244 Da, Table 1). The LAT1-utilizing prodrugs were then synthesized by conjugating L-Phe at the meta position to the carboxylic group of the parent drug via an amide bond, as described above and previously reported.<sup>20</sup> One known factor that limits the brain exposure to CNS drugs is the high plasma protein binding that decreases the unbound fraction of the drugs in plasma. NSAIDs are known to be extensively bound to plasma proteins as reported earlier<sup>37</sup> and also shown here (Table 1), which limits their brain uptake. The prodrugs were less bound to the mouse plasma proteins than their parent drugs (Table 1). Because the ionized acids were shown to be highly bound to plasma proteins,<sup>38</sup> conjugating the acidic parent drugs with the neutral phenylalanine could explain the decrease in the plasma protein binding between the prodrugs and their parent drugs.

**3.2. Membrane Transporters in the Immortalized Human Microglia.** To investigate whether the drug delivery via LAT1 utilization can also be applied to human brain cells, we studied the expression and function of LAT1 in SV40 cells. We found that both LAT1/4F2hc subunits were expressed in the crude and plasma membranes of SV40 cells. However, the LAT1 expression levels were almost 4-fold higher in primary mouse astrocytes and BV2<sup>12</sup> than in the human SV40 cells, which was in agreement with the human-to-mouse LAT1 ratio in the brain microvessels.<sup>39</sup> The transporters detected in the crude membrane fraction were enriched in the plasma membrane fraction except for 4F2hc protein. This indicates that these transporters, except for 4F2hc protein, were mainly expressed in the plasma membranes of the SV40 cells. Moreover, SV40 cells expressed ASCT1, a transporter for small neutral amino acid, which supposedly will not affect the function of LAT1 that transports large neutral amino acids. Besides, the expression of the three quantified OATPs and ASCT2 were very low or under the detection limits. Thus, SV40 cells expressed a functional LAT1 transporter as indicated by the selective transport of the natural LAT1 substrate (L-Leu) across the plasma membrane (Figure 1B–D), and this transport was inhibited by the selective LAT1 inhibitor.<sup>24</sup> Nevertheless, SV40 cells also expressed the multidrug resistance-associated protein 1 (MRP1), which may interact with NSAIDs as previously proposed in the literature.<sup>40</sup>

**3.3. Uptake Kinetics in the Human and Mouse Brain Cells.** The target enzymes (cyclooxygenases) of NSAIDs are located intracellularly in the brain parenchymal cells,<sup>41</sup> as it is the case for many other CNS drug targets. Thus, it is essential to

Table 4. Pharmacokinetic Parameters of the Studied Compounds

PK parameter	prodrug bioconversion		prodrug bioconversion		prodrug bioconversion		prodrug bioconversion			
	FLB <sup>a</sup>	PD <sup>b</sup> 1	SA <sup>c</sup>	PD 2	IBU <sup>d</sup>	PD 3	NAP <sup>e</sup>	PD 4	NAP released	ratio to NAP
AUC <sub>plasma</sub> (min × nmol/mL)	28 734	3240	2474	3510	8075	6136	18 332	1809	741	0.04
AUC <sub>brain</sub> (min × nmol/g tissue)	178	60	71.7	66.5	139.3	15.5	113.1	50.2	66.0	0.58
AUC <sub>liver</sub> (min × nmol/g tissue)	2731	32 284	554	2120	1578	9046	1071	19 516	ND	ND
AUC <sub>brain/plasma</sub> (K <sub>p,brain</sub> )	0.006	0.019	0.029	0.019	0.017	0.003	0.006	0.028	0.004	0.67
AUC <sub>brain/liver</sub>	0.065	0.002	0.129	0.031	0.088	0.002	0.106	0.003	ND	ND
AUC <sub>liver/plasma</sub>	0.095	9.96	0.224	0.604	0.195	1.47	0.058	10.8	ND	ND
K <sub>p,brain</sub>	0.638	1.737	4.084	0.023	19.164	0.014	5.14	0.203	2.999	0.58
K <sub>p,brain/liver</sub>	9.80	931	31.6	0.73	217.14	8.29	48.7	79.1	ND	ND
C <sub>max</sub> plasma (nmol/mL)	163	176	54.6	162	115	173	205	109	3.35	0.02
t <sub>max</sub> plasma (min)	30	5	10	10	5	10	5	5	120	ND
t <sub>1/2</sub> plasma (min)	167	113	21	30	73	57	108	97	ND	ND
V <sub>Z/F</sub> (L/kg)	0.15	1.18	0.30	0.37	0.28	0.44	0.18	1.94	0.65	0.44
C <sub>max</sub> brain (nmol/g tissue)	1.32	0.52	1.28	1.2	2.66	0.23	1.48	0.59	0.65	0.44
t <sub>max</sub> brain (min)	10	10	30	30	10	2	10	5	10	ND
t <sub>1/2</sub> brain (min)	194	ND	24	80	70	ND	148	88	88	ND
C <sub>max</sub> liver (nmol/g tissue)	21.2	154	15.6	38.9	34.8	55.6	22.1	132	ND	ND
t <sub>max</sub> liver (min)	10	100	10	30	5	60	5	30	ND	ND
t <sub>1/2</sub> liver (min)	213	ND	21	48	61	116	96	108	ND	ND

<sup>a</sup>FLB = flurbiprofen. <sup>b</sup>PD = prodrug. <sup>c</sup>SA = salicylic acid. <sup>d</sup>IBU = ibuprofen. <sup>e</sup>NAP = naproxen. <sup>f</sup>ND = not detected.

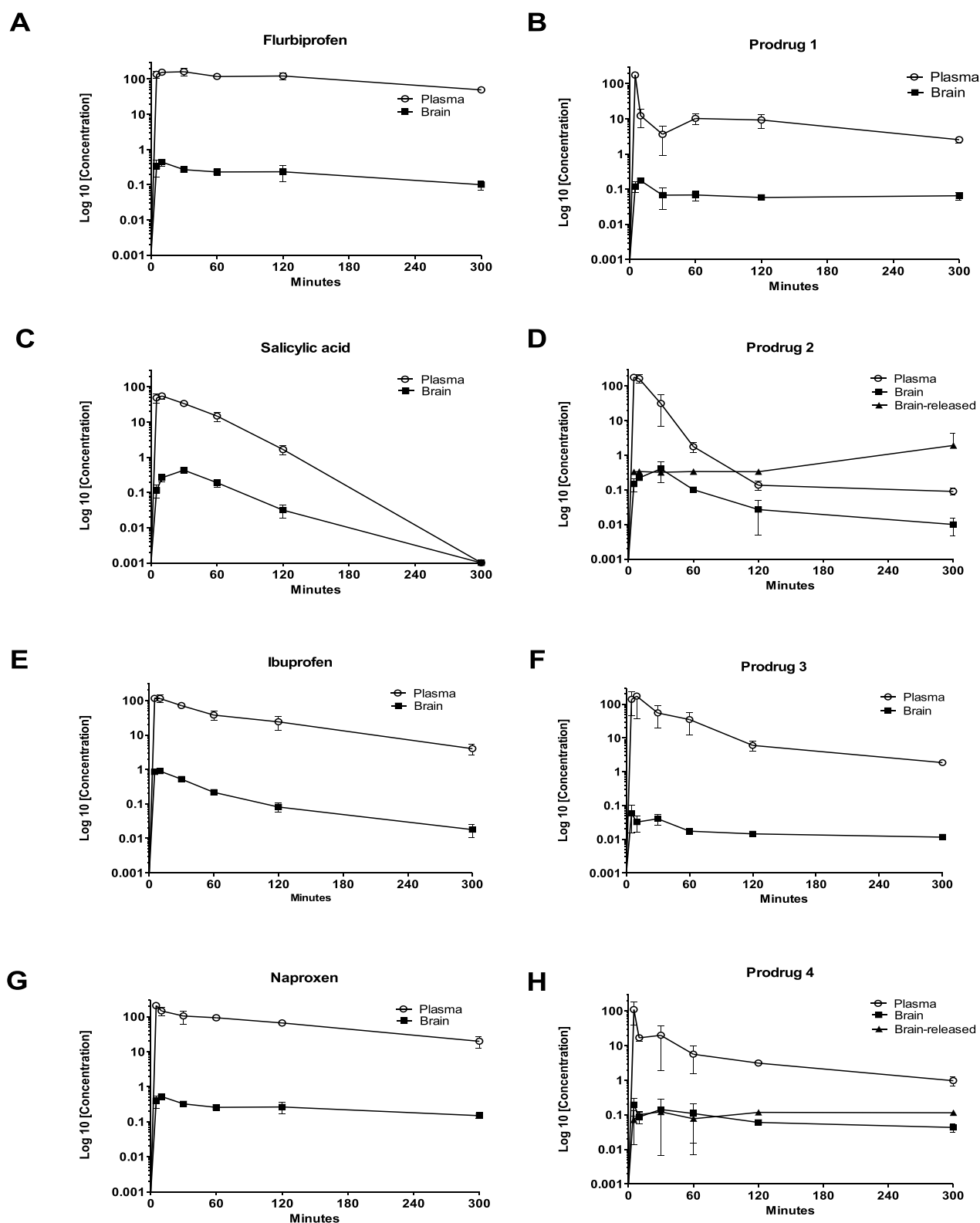


**Figure 3.** Total tissue concentrations of flurbiprofen (A), prodrug 1 (B), salicylic acid (C), prodrug 2 (D), ibuprofen (E), prodrug 3 (F), naproxen (G), and prodrug 4 (H) in the mouse brain as nmol/g tissue (■) and in the mouse plasma as nmol/mL (○) and the concentration of parent drugs released from the prodrugs in the brain as nmol/g tissue (▲). The results are expressed as mean  $\pm$  SD ( $n = 3$ ).

deliver the CNS drugs not only across the BBB but also into their target sites in the brain. Therefore, we examined here the cellular kinetics of the prodrugs in the primary mouse astrocytes and BV2 cells as well as in the human immortalized microglia cells (SV40). The competitive ligand-binding assays using known

LAT1 substrate or inhibitor give information about the LAT1 utilization, while the total cellular uptake shows the transport's capacity and detect if there are other secondary transporters.

**3.3.1. LAT1 Utilization in the Cultured Brain Cells.** All the prodrugs were able to compete with [ $^{14}$ C]-L-Leu for LAT1

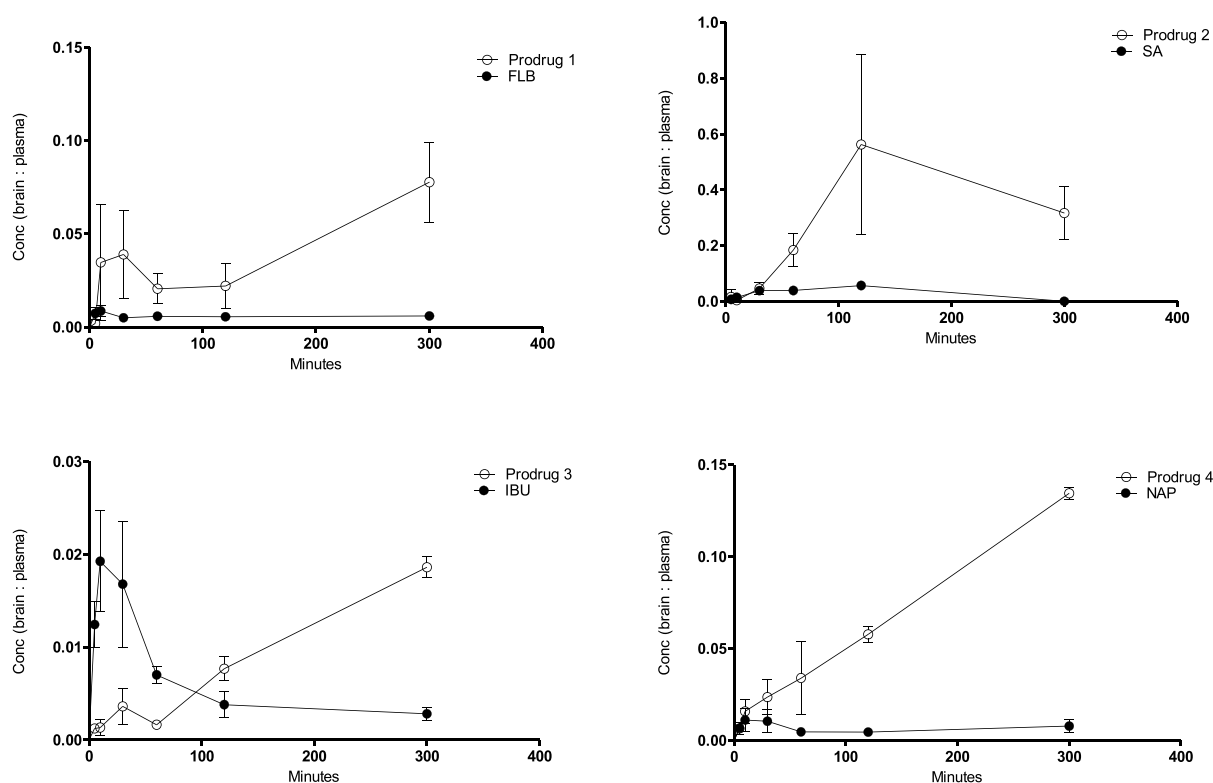


**Figure 4.** Brain-to-plasma concentration ratios of prodrugs (○) and their parents (●) in mice. The results are expressed as mean  $\pm$  SD ( $n = 3$ ).

utilization. The prodrugs showed high potency to utilize LAT1 in all the cell types with  $IC_{50}$  values in the low micromolar range (3–54  $\mu$ M) (Table 3). This finding confirms not only that the prodrugs can utilize LAT1 even in the presence of a natural amino acid as previously reported<sup>12,20</sup> but also that this approach can be applied to noncancer human brain cells (SV40). Additionally, the Michaelis-Menten affinity constants ( $K_m$ ) further confirmed the high LAT1 utilization of the prodrugs when compared with that of L-Leu (Table 4).

**3.3.2. LAT1 Transport Capacity.** The transport capacity or the ability of the drugs to accumulate into the cells is another parameter to determine the optimal drug uptake. The prodrugs were transported efficiently into all the cell types after the 30 min incubation. However, the NSAID parent drugs were not detected in all the cell types, which is probably because of the efflux transporters such as MRP1 that is expressed in SV40 cells (Figure 1). Most prodrugs showed a secondary transport system at only the higher concentrations ( $>50 \mu$ M). This secondary transport system is characterized by being low-affinity and high-capacity transporter(s) as it is only activated when LAT1 is saturated at high concentrations (supplementary data, Figures S5, S6, and S7). The prodrugs showed different transport capacities via LAT1; prodrugs 1 and 2 were transported in higher quantities than prodrugs 3 and 4. However, the exceptional high uptake of prodrug 3 in SV40 cells ( $V_{max} \approx 75$  pmol/(min  $\times$  mg protein)) might be due to another secondary transporter that is not expressed in mouse astrocytes and BV2 cells. Thus, prodrugs 3 and 4 were not efficiently transported from the LAT1 recognizing cavity, and they were better binders rather than substrates of LAT1. This also explains why the LAT1 inhibitor was able to block the uptake of prodrugs 1 and 2 but not prodrugs 3 and 4 in all the cell types.

Taking the LAT1 utilization and transport capacity together, prodrugs 1 and 2 showed promising uptake properties. Both

prodrugs are transported into all the cultured cell types with high affinity and high transport capacity. However, prodrugs 3 and 4 showed higher affinity for LAT1 but low transport capacity. This indicates that the parent drug moiety may affect the transport capacity but not the affinity of LAT1 utilization.

**3.4. Pharmacokinetic Study in Mice.** While the cellular uptake of the prodrugs into the brain cells was promising, it is essential to determine how the prodrugs are distributing centrally and peripherally in mice. After an i.p. dose of 25  $\mu$ mol/kg, the concentrations of the prodrugs and their parent drugs were followed in the brain, liver, and plasma over a period of 5 h. The peak concentrations in plasma ( $C_{max}$ ) varied considerably between the parent drugs, ranging from 55 to 205 nmol/mL. This indicates differences in the diffusion properties of the parent drugs from the intraperitoneal cavity into the systemic circulation. In contrast, the prodrugs showed small differences in their plasma  $C_{max}$  values (109–176 nmol/mL) (Table 4). This suggests that the model of LAT1 utilization showed somehow consistent diffusion properties regardless of the different parent drug moiety. Nevertheless, the distribution of the prodrugs in mice and the in vivo release of the parent drugs varied markedly.

The prodrugs, as amide conjugates of their parent drugs, are expected to be stable in vivo. This was particularly true in the mouse liver, as no parent drugs were detected or the release was just under the detection limits, which would also be negligible in that case. However, the amide prodrugs can release their parent drugs due to the enzymatic actions of carboxylesterases, peptidases, or proteases.<sup>42</sup> In the mouse plasma, prodrugs 1, 2, and 4 released their parent drugs but in very small amounts (0.7–4%), while prodrug 3 was particularly unstable with 26% delayed release of its parent drug IBU. Additionally, the peak concentration of the released parent drug was detected at the 2 h time point in the cases of prodrugs 3 and 4, at the 5 h time point

in the case of prodrug 1, and at the 10 min time point in the case of prodrug 2 (see  $T_{\max, \text{plasma}}$  Table 4). Most importantly, prodrug 2 released a significant amount of its parent drug SA in the mouse brain, which was estimated as 5 times higher than the amount that reached the brain after the SA dosing itself. Similarly, prodrug 4 released NAP in the mouse brain in an amount estimated as half the amount that reached the brain after the NAP dosing itself.

The brain-to-plasma partition coefficients such as  $K_{p, \text{brain}}$  and  $K_{p, u, \text{brain}}$  explained the brain delivery of the prodrugs as compared to that of their parent drugs. Prodrug 2 improved the brain exposure of its parent drug SA as demonstrated by the 5 times higher  $K_{p, u, \text{brain}}$  value than that of SA itself. Additionally, the total brain exposure of prodrug 4 was supposedly improved 4.5-fold over its parent drug as demonstrated by its  $K_{p, \text{brain}}$  value. However, the distribution of prodrug 4 into the mouse brain was limited due to the unspecific protein binding (Table 1). The  $K_{p, u, \text{brain}}$  of NAP was higher than the combined values of prodrug 4 and the released NAP in the mouse brain (Figure 3 and Table 4). Nevertheless, both prodrugs 2 and 4 released their parent drugs specifically in the mouse brain and not in the periphery (plasma or liver). Hence, prodrugs 2 and 4 delivered not only their parent drugs into the brain but also minimized their peripheral exposure, as previously reported.<sup>20</sup> On the other hand, prodrug 1 was not able to improve the brain delivery of its parent drug FLB despite its high LAT1 affinity and transport capacity. This could be mainly explained by the high nonspecific protein binding in the mouse plasma and liver (Table 1). Thus, a small fraction is only free in the plasma to diffuse into the brain. Similarly, the unexpected instability of prodrug 3 in the mouse plasma makes it difficult to speculate its brain delivery (Table 4).

## 4. EXPERIMENTAL SECTION

All reagents and materials used in the analytical analysis were commercial of high purity analytical grade or ultrapure HPLC grade purchased from Sigma (St. Louis, MO, USA), Acros Organics (Waltham, MA, USA), or Merck (Darmstadt, Germany). Water was purified using a Milli-Q Gradient system (Millipore, Milford, MA, USA).

**4.1. General Synthetic Procedures.** The reactions were monitored by thin-layer chromatography using aluminum sheets coated with silica gel 60 F<sub>245</sub> (0.24 mm) with suitable visualization. Purifications by flash chromatography were performed on silica gel 60 (0.063–0.200 mm mesh). <sup>1</sup>H and <sup>13</sup>C nuclear magnetic resonance (NMR) spectra were recorded on a Bruker Avance 500 spectrometer (Bruker Biospin, Fällanden, Switzerland) operating at 500.13 and 125.75 MHz, respectively, using tetramethylsilane as an internal standard. ESI-MS spectra were recorded by a Finnigan LCQ quadrupole ion trap mass spectrometer (Finnigan MAT, San Jose, CA, USA) equipped with an electrospray ionization source. Over 95% purities were confirmed for the final products by elemental analysis (C, H, N) with a PerkinElmer 2400 Series II CHNS/O organic elemental analyzer (PerkinElmer Inc., Waltham, MA, USA).

**4.2. General Procedure for Preparing Prodrugs 1–4.** Prodrugs 1–4 were prepared according to the literature procedure.<sup>21</sup> SA, FLB, IBU, or NAP (0.71–2.17 mmol) in anhydrous CH<sub>2</sub>Cl<sub>2</sub> (10–20 mL) was reacted with SOCl<sub>2</sub> (1.07–4.34 mmol) in a microwave reactor (Biotage Initiator, Biotage AB, Uppsala, Sweden) at 100 °C for 60 min under Ar atm. The reaction mixture was evaporated, and the residue was redissolved in CH<sub>2</sub>Cl<sub>2</sub> (10–20 mL) and reacted with *t*-Boc-3-amino-*L*-phenylalanine (0.71–2.17 mmol) in the presence of powdered NaOH (1.43–4.34 mmol) at room temperature (RT) under Ar atm overnight.<sup>21</sup> The solvent was removed, and the residue was purified by flash column chromatography eluting with 1–30% MeOH/CH<sub>2</sub>Cl<sub>2</sub> to yield the prodrug intermediates (44–88%).

The intermediates (0.49–2.86 mmol) were dissolved in anhydrous CH<sub>2</sub>Cl<sub>2</sub> (ca. 10 mL) and reacted with trifluoroacetic acid (1–2 mL) by stirring the reaction mixture at RT overnight. The solvents were removed, and the residue was redissolved in THF and stirred with 1 M HCl (2–4 mL) at RT for 30 min. The mixture was evaporated, and the residue was purified by flash column chromatography eluting with 1–99% MeOH/CH<sub>2</sub>Cl<sub>2</sub> to yield the prodrugs 1–4 as off-white solids (51–74%).

**4.2.1. (2*S*)-2-Amino-3-(3-(2-(2-fluoro-[1,1'-biphenyl]-4-yl)propanamido)phenyl)propanoic Acid 1.** <sup>1</sup>H NMR (500 MHz, (CD<sub>3</sub>)<sub>2</sub>SO): δ ppm 10.12 (d, *J* = 13.25 Hz, 1H), 7.59–7.50 (m, 3H), 7.50–7.44 (m, 4H), 7.40–7.33 (m, 2H), 7.31 (s, 1H), 7.19 (t, *J* = 7.7 Hz, 1H), 6.95 (d, *J* = 7.5 Hz, 1H), 3.98 (q, *J* = 6.8 Hz, 1H), 3.47–3.42 (m, 1H), 3.15–3.08 (m, 1H), 2.88–2.79 (m, 1H), 1.44 (d, *J* = 6.9 Hz, 3H). <sup>13</sup>C NMR (125 MHz, (CD<sub>3</sub>)<sub>2</sub>SO): δ ppm 171.60, 169.59, 159.79 (*J* = 245.8 Hz), 143.87 (*J* = 8.2 Hz), 139.20, 138.03 (*J* = 7.2 Hz), 134.93, 130.60 (*J* = 3.5 Hz), 128.69 (*J* = 2.5 Hz, 2C), 128.58 (2C), 127.73, 126.58 (*J* = 13.4 Hz), 124.28, 123.85 (*J* = 3.0 Hz), 120.10, 117.48, 115.09, 114.82, 55.36, 45.23, 37.03, 18.34. MS (ESI–) for C<sub>24</sub>H<sub>22</sub>FN<sub>2</sub>O<sub>3</sub> (M – H)<sup>–</sup>: calcd 405.45, found 405.10. Anal. calcd for (C<sub>24</sub>H<sub>22</sub>FN<sub>2</sub>O<sub>3</sub> × 1.0 CH<sub>2</sub>Cl<sub>2</sub>): C, 61.11; H, 4.92; N, 5.70; found = C, 61.12; H, 5.15; N, 5.85.

**4.2.2. (5*S*)-2-Amino-3-(3-(2-hydroxybenzamido)phenyl)propanoic Acid 2.** <sup>1</sup>H NMR (500 MHz, (CD<sub>3</sub>)<sub>2</sub>SO): δ ppm 10.78 (s, 1H), 8.00 (d, *J* = 8.1 Hz, 1H), 7.67 (d, *J* = 8.2 Hz, 1H), 7.52 (s, 1H), 7.38 (t, *J* = 8.2 Hz, 1H), 7.26 (t, *J* = 7.8 Hz, 1H), 7.04 (d, *J* = 7.5 Hz, 1H), 6.98 (d, *J* = 8.2 Hz, 1H), 6.91 (t, *J* = 7.6 Hz, 1H), 3.49–3.67 (m, 1H), 3.21–3.19 (m, 1H), 2.92–2.88 (m, 1H). <sup>13</sup>C NMR (125 MHz, (CD<sub>3</sub>)<sub>2</sub>SO): δ ppm 172.98, 166.16, 158.78, 138.17, 138.03, 133.39, 129.10, 128.51, 125.04, 121.62, 119.07, 118.62, 117.29, 117.27, 55.44, 36.95. MS (ESI–) for C<sub>16</sub>H<sub>15</sub>N<sub>2</sub>O<sub>4</sub> (M – H)<sup>–</sup>: calcd 299.30, found 299.15. Anal. calcd for (C<sub>16</sub>H<sub>15</sub>N<sub>2</sub>O<sub>4</sub> × 1.09 EtOH): C, 62.29; H, 6.48; N, 7.99; found = C, 62.73; H, 6.15; N, 7.55.

**4.2.3. (2*S*)-2-Amino-3-(3-(2-(4-isobutylphenyl)propanamido)phenyl)propanoic Acid 3.** <sup>1</sup>H NMR (500 MHz, (CD<sub>3</sub>)<sub>2</sub>SO): δ ppm 10.14 (d, *J* = 8.0 Hz, 1H), 7.55–7.46 (m, 2H), 7.29 (d, *J* = 7.1 Hz, 2H), 7.18 (t, *J* = 7.7 Hz, 1H), 7.09 (d, *J* = 7.1 Hz, 2H), 6.93 (d, *J* = 7.4 Hz, 1H), 3.87–3.80 (m, 1H), 3.51–3.45 (m, 1H), 3.14–3.06 (m, 1H), 2.86–2.79 (m, 1H), 2.39 (d, *J* = 7.0 Hz, 2H), 1.79 (hept, *J* = 6.7 Hz, 1H), 1.38 (d, *J* = 6.9 Hz, 3H), 0.84 (d, *J* = 6.5 Hz, 6H). <sup>13</sup>C NMR (125 MHz, (CD<sub>3</sub>)<sub>2</sub>SO): δ ppm 172.36, 169.75, 139.40, 139.37, 139.21, 137.79, 128.85 (2C), 128.58, 127.01 (2C), 124.08, 119.99, 117.46, 55.25, 45.40, 44.22, 36.96, 29.59, 22.17 (2C), 18.62. MS (ESI–) for C<sub>22</sub>H<sub>27</sub>N<sub>2</sub>O<sub>3</sub> (M – H)<sup>–</sup>: calcd 367.47, found 367.20. Anal. calcd for (C<sub>22</sub>H<sub>28</sub>N<sub>2</sub>O<sub>3</sub> × 1.4 CH<sub>2</sub>Cl<sub>2</sub> × 0.4 MeOH): C, 57.15; H, 6.25; N, 5.60; found = C, 56.92; H, 6.52; N, 5.72.

**4.2.4. (2*S*)-2-Amino-3-(3-(2-(6-methoxynaphthalen-2-yl)propanamido)phenyl)propanoic Acid 4.** <sup>1</sup>H NMR (500 MHz, (CD<sub>3</sub>)<sub>2</sub>SO): δ ppm 10.20 (s, 1H), 7.83–7.75 (m, 3H), 7.56–7.48 (m, 3H), 7.26 (s, 1H), 7.20–7.13 (m, 2H), 6.92 (d, *J* = 7.7 Hz, 1H), 4.00 (q, *J* = 7.0 Hz, 1H), 3.85 (s, 3H), 3.45–3.40 (m, 1H), 3.14–3.07 (m, 1H), 2.83–2.77 (m, 1H), 1.48 (d, *J* = 6.9 Hz, 3H). <sup>13</sup>C NMR (125 MHz, (CD<sub>3</sub>)<sub>2</sub>SO): δ ppm 172.29, 169.57, 157.03, 139.33, 137.98, 137.07, 133.19, 129.11, 128.57, 128.35, 126.71, 126.39, 125.39, 124.11, 120.05, 118.62, 117.47, 105.68, 55.39, 55.13, 45.73, 37.04, 18.63. MS (ESI–) for C<sub>23</sub>H<sub>23</sub>N<sub>2</sub>O<sub>4</sub> (M – H)<sup>–</sup>: calcd 391.45, found 391.20. Anal. calcd for (C<sub>23</sub>H<sub>23</sub>N<sub>2</sub>O<sub>4</sub> × 1.1 CH<sub>2</sub>Cl<sub>2</sub>): C, 59.58; H, 5.21; N, 5.77; found = C, 59.36; H, 5.57; N, 5.69.

**4.3. Physicochemical Properties and Nonspecific Protein Binding.** The unbound fractions of the studied compounds were determined in mouse serum as well as in the S9 subcellular fractions of the mouse liver and brain by using Rapid Equilibrium Dialysis (RED) plates (Thermo Fisher Scientific, Inc., Waltham, MA, USA). Briefly, the studied compounds (10 μM) were spiked to 100 μL of mouse S9 subcellular fraction or serum and added to the reaction chamber. A total of 350 μL of HBSS buffer was added to the buffer chamber of the RED plate. The dialysis plate was incubated at 37 °C for 4 h while shaking. A total of 50 μL of samples was taken from the reaction and buffer chambers, and equal amounts of buffer or blank homogenate were added, respectively, to yield identical matrices. The samples were

treated with 100  $\mu\text{L}$  of ice-cold ACN (including the selected internal standards) to precipitate the proteins, and the supernatants were collected for LC–MS analysis after centrifugation at  $12\,000 \times g$  for 10 min. The unbound drug fraction ( $f_{u,\text{tissue}}$ ) was calculated and corrected with the homogenate dilution factor ( $D$ ), as described by Kalvass et al.<sup>43</sup> Additionally,  $\text{cLogD}_{\text{pH}7.4}$  values of the studied compounds were predicted using MarvinSketch, ChemAxon software.

**4.4. Chemical and Enzymatic Stabilities of the Prodrugs.** The control mouse brain and liver were collected freshly and homogenized with Omni Bead Ruptor 24 Elite homogenizer (Omni International, Kennesaw, GA, USA) in (1:4 w/v) 50 mM Tris-buffered saline (TBS) (pH 7.4). The brain and liver homogenates were centrifuged at  $9\,000 \times g$  for 20 min at 4 °C to prepare the S9 subcellular fractions. The mouse blood was aseptically collected from control animals, while the human plasma was supplied from the Finnish Red Cross as freshly frozen (Helsinki, Finland). Then, the mouse plasma was prepared by centrifugation at  $1200 \times g$  for 10 min at 4 °C. The protein concentrations were measured for each homogenate by Bio-Rad Protein Assay, based on the Bradford dye-binding method (EnVision, PerkinElmer, Inc., Waltham, MA, USA).

The bioconversion and stability of the prodrugs were determined in mouse brain, S9 subcellular fractions of mouse or human liver (Sigma-Aldrich, St. Louis, MO, USA), and mouse or human plasma. A total amount of 100  $\mu\text{M}$  prodrugs in 2% DMSO were incubated with 1 mg/mL protein of the above-mentioned homogenates at 37 °C. Aliquots of 100  $\mu\text{L}$  were taken from the incubation mixture at appropriate intervals. Then, the reaction was stopped, and the proteins were precipitated by adding 100  $\mu\text{L}$  of ice-cold acetonitrile (ACN). The samples were then centrifuged at  $12\,000 \times g$  for 5 min at RT, and the supernatants were collected and analyzed by LC–MS/MS methods described in the *Liquid Chromatography–Tandem Mass Spectrometry Analysis* section. In the blank reactions (chemical stability), the biological material was replaced with the same volume of buffer. Because pseudo-first-order half-lives ( $t_{1/2}$ ) of bioconversion were not calculated due to the relatively high stability of the prodrugs in vitro, the degradation was reported herein as percentages (%), calculated as the difference in drug concentrations between the last (6 or 24 h) and the first (0 h) time points.

**4.5. Cultured Cells.** Primary astrocytes were isolated from cortices of two-day-old C57BL/6 wild type mice as previously described.<sup>12,44,45</sup> The cells were cultured in DMEM (+ 4500 mg/L glucose, + L-glutamine, + pyruvate; Gibco-BRL) supplemented with 10% heat-inactivated fetal bovine serum (GIBCO, MD, USA) and 100 U/mL penicillin and streptomycin (EuroClone, Milan, Italy).

Immortalized BV2 cells were a generous gift from Prof. Mikko Hiltunen, while SV40 cells were originated from Tardieu lab<sup>46</sup> and were a kind gift from Dr. Dora Brites and Prof. Tarja Malm. Both cell lines were cultured in RPMI-1640 medium containing L-glutamine (2 mM), heat-inactivated fetal bovine serum (10%), penicillin (50 U/mL), and streptomycin (50  $\mu\text{g}/\text{mL}$ ). The experiments were done using cell passaging numbers between 9 and 13.

**4.6. Membrane Transporters in the Immortalized Human Microglia.** The LAT1/4F2hc transporter was quantified in the crude and plasma membrane fractions of SV40 cells using a triple quadrupole mass spectrometer (MSD 6495, Agilent Technologies, Santa Clara, CA, USA) following the targeted proteomic approach. Additionally, other influx and efflux transporters such as GLUT1,  $\text{Na}^+/\text{K}^+$  ATPase, ASCT1, ASCT2, OATP1A2, OATP2B1, OATP1B3, MRP1, and MRP4 were quantified from the same samples. Briefly, the cellular fractions were enzymatically digested into peptides, and a marker peptide for each protein was selected based on the protocol described by ref 47 and validated by ref 48. Thereafter, the proteins were quantified using the selected/multiple reaction monitoring (SRM/MRM) mode of at least three transitions derived from the isotopically labeled and quantified peptides (JPT Peptide Technologies GmbH, Berlin, Germany). The proteins were then quantified based on the ratio between the endogenous digested peptides and the heavy-labeled peptides (supplementary data, Table S2).

**4.6.1. Extraction and Digestion of Membrane Proteins.** The SV40 cells were obtained from ten confluent culture plates per one replicate

using a cell scraper and centrifuged at  $250 \times g$  at 4 °C for 5 min. The crude and plasma membrane fractions were isolated from the cells using the membrane protein extraction kit (BioVision Incorporated, Milpitas, CA, USA) by following the manufacturer's protocol. The protein concentration was measured by Bio-Rad Protein Assay, based on the Bradford dye-binding method (EnVision, PerkinElmer, Inc., Waltham, MA, USA).

The membrane fractions were denatured, reduced, and S-carboxymethylated before the digestion with LysC (Sigma-Aldrich, St. Louis, MO, USA) and TPCK-trypsin (Promega Biotech AB, Nacka, Sweden). Briefly, a total amount of 50  $\mu\text{g}$  of protein was mixed with denaturing solution containing 7 M Guanidine hydrochloride, 0.5 M Tris-HCl and 10 mM EDTA-Na. Thereafter, the proteins were reduced by dithiothreitol (1:50, w/w) and S-carboxymethylated by iodoacetamide (1:20, w/w) (Sigma-Aldrich, St. Louis, MO, USA). The alkylated proteins were precipitated by methanol/chloroform/water (4:1:3) and centrifuged at  $18\,000 \times g$  for 5 min at 4 °C. The pellet was then resuspended in 6 M urea and mixed for 10 min at room temperature. The samples were then diluted with 0.1 M Tris-HCl to a final concentration of 1.2 M urea and dissolved completely by intermittent sonication (Branson 3510, Danbury, CT, USA). The dissolved proteins were first digested with LysC (1/100, w/w) (Sigma-Aldrich, St. Louis, MO, USA) and 0.05% ProteaseMax (Promega Biotech AB, Nacka, Sweden) for 3 h at room temperature. Then, the samples were spiked with 10  $\mu\text{L}$  (30 fmol) of the labeled peptides for absolute quantification (JPT Peptide Technologies GmbH, Berlin, Germany) (supplementary data, Table S2). The samples were further incubated with (1/100, w/w) TPCK-Trypsin (Promega Biotech AB, Nacka, Sweden) for 18 h at 37 °C. The tryptic digestion was then quenched by adding 40  $\mu\text{L}$  of 5% formic acid. The samples were then centrifuged at  $18\,000 \times g$  for 5 min at 4 °C, and the supernatant was transferred to HPLC vial for the analysis.

**4.6.2. LC–MS/MS–Selective Reaction Monitoring (SRM) Targeted Protein Quantification.** The digested peptides were analyzed using a UPLC system coupled with a triple quadrupole mass spectrometer with a heated electrospray ionization source in the positive mode (UPLC 1290 and MSD 6495, Agilent Technologies, Santa Clara, CA, USA). A total amount of 20  $\mu\text{L}$  of the digested peptides (10  $\mu\text{g}$ ) was separated using AdvanceBio Peptide Map 2.1  $\times$  250 mm, 2.7  $\mu\text{m}$  column (Agilent Technologies, Santa Clara, CA, USA) and LC eluents of 0.1% formic acid in water (A) and acetonitrile (B). The peptides were eluted following a constant flow rate of 0.3 mL/min and a gradient of 2–7% B for 2 min, followed by 7–30% B for 48 min, 30–45% B for 3 min, and 45–80% B for 2.5 min before re-equilibrating the column again for 4.5 min. Data was acquired using Agilent MassHunter Workstation Acquisition and processed using Skyline software 20.1.

**4.7. LAT1 Utilization in the Cultured Cells.** The uptake of the prodrugs (25, 50, 100  $\mu\text{M}$ ) and [ $^{14}\text{C}$ ]-L-Leu (0.76  $\mu\text{M}$ ) were quantified in astrocytes, BV2, and SV40 cells in the presence and absence of the selective LAT1 inhibitor (KMH-233).<sup>24</sup> First, the LAT1 inhibitor (100  $\mu\text{M}$ ) or HBSS were preincubated with the cells for 10 min. Thereafter, the preincubation mixture was removed, and the prodrugs or [ $^{14}\text{C}$ ]-L-Leu were added in the presence of the LAT1 inhibitor or HBSS for 30 min. The incubation mixture was then aspirated, and the cells were washed and lysed for 1 h with 0.1 M NaOH (250  $\mu\text{L}$ ) and stored at –20 °C prior to the analysis with the LC–MS/MS method as described in the *Liquid Chromatography–Tandem Mass Spectrometry Analysis* section.

The ability of the prodrugs to inhibit uptake [ $^{14}\text{C}$ ]-L-Leu was studied in the primary astrocytes, BV2, and SV40 cells. Cells were incubated for 5 min with 0.1–1000  $\mu\text{M}$  prodrugs and 0.76  $\mu\text{M}$  [ $^{14}\text{C}$ ]-L-Leu (PerkinElmer, Waltham, MA, USA) in HBSS. After washing the cells with HBSS, the cells were lysed with 0.1 M NaOH (250  $\mu\text{L}$ ), and the lysates were mixed with 1 mL of emulsifier cocktail (PerkinElmer, Waltham, MA, USA). The radioactivity of the cell lysates was measured by a liquid scintillation counter (MicroBeta2, PerkinElmer, MA, USA). The concentrations at which 50% of the uptake is inhibited ( $\text{IC}_{50}$ ) were determined for each compound using GraphPad Prism 5.

**4.8. LAT1 Transport Capacity in the Cultured Cells.** The cells were seeded at a density of  $1 \times 10^5$  cells/well onto 24-well plates 1 day

before the uptake experiments. The culture media was aspirated, and the cells were washed with prewarmed HBSS solution (Hank's balanced salt solution) containing 125 mM choline chloride, 4.8 mM KCl, 1.2 mM  $\text{MgSO}_4$ , 1.2 mM  $\text{KH}_2\text{PO}_4$ , 1.3 mM  $\text{CaCl}_2$ , 5.6 mM glucose, and 25 mM HEPES (pH 7.4 adjusted with 1 M NaOH). A total of 500  $\mu\text{L}$  of prewarmed HBSS was preincubated with the cells at 37 °C for 10 min before adding the studied compounds. Different concentrations of the studied compounds (1–200  $\mu\text{M}$ ) were diluted in HBSS (250  $\mu\text{L}$ ) and incubated with the cells for 30 min in RT. The reaction was stopped by removing the incubation medium and adding 500  $\mu\text{L}$  of ice-cold HBSS, and the cells were washed twice with HBSS on ice. Thereafter, the cells were lysed for 1 h with 0.1 M NaOH (250  $\mu\text{L}$ ) and stored at –20 °C prior to the analysis with the LC–MS/MS method as described in the [Liquid Chromatography–Tandem Mass Spectrometry Analysis](#) section.

**4.9. Pharmacokinetic Studies in Mice.** Eight-week-old male healthy mice (C57BL/6JOLAHSd) weighing  $30 \pm 5$  g were purchased from Envigo, Netherlands. Animals were housed in well-ventilated stainless-steel cages with ad-libitum consumption of tap water and food pellets (Teklad 2016, Envigo), temperature of  $22 \pm 2$  °C, relative humidity of  $55 \pm 15\%$ , and 12/12 h light–dark cycle. The procedures were conducted under a license (ESAVI-2015-003347) approved by the Finnish National Animal Experiment Board and in accordance with the European Community Guidelines and Guide for the Care and Use of Laboratory Animals. All effort was taken to minimize the number of animals used and their suffering. Stock solutions (80 mM) of the studied compounds were prepared in DMSO 1 day before the study and were dosed to animals as a solution in normal saline via intraperitoneal (i.p.) bolus administration (25  $\mu\text{mol}/\text{kg}$ ), while the DMSO final concentration was 3%. The mice were anaesthetized using a mixture of ketamine (140 mg/kg) and xylazine (8 mg/kg) (Intervet International, Netherlands) prior to the transcardial perfusion of ice-cold physiological saline for 1 min. Blood (for preparation of plasma), liver, and brain samples were collected at 5, 10, 30, 60, 120, and 300 min after injection. Brain and liver samples were immediately snap-frozen in liquid nitrogen and stored at –80 °C. Blood samples were immediately vortexed with 1  $\mu\text{L}$  of 1000 IU heparin and centrifuged at  $1500 \times g$  for 10 min at 4 °C. Finally, the supernatants (plasma) were stored at –80 °C.

**4.10. Liquid Chromatography–Tandem Mass Spectrometry Analysis.** **4.10.1. Sample Preparation.** The cell lysates were diluted (1:4, v/v) and acidified with 0.1% formic acid in ACN and centrifuged at  $18000 \times g$  for 10 min at 4 °C. For the uptake studies, the drug concentrations were calculated from a calibration curve (1–2500 nM) prepared the same way as the samples by spiking known standard concentrations to control cell lysates. The protein concentrations on each plate were determined as the mean of three samples by Bio-Rad Protein Assay, based on the Bradford dye-binding method (EnVision, PerkinElmer, Inc., Waltham, MA, USA). The uptake results were then normalized to the protein content and presented as pmol/(min  $\times$  mg protein). Michaelis–Menten kinetic parameters ( $V_{\text{max}}$  and  $K_m$ ) were calculated using GraphPad Prism 5, where  $K_m$  is the concentration that gives half of the maximum uptake concentration ( $V_{\text{max}}$ ).

The frozen mouse plasma was first melted in wet ice. A total of 25  $\mu\text{L}$  was mixed carefully with 75  $\mu\text{L}$  of ACN acidified with 0.1% formic acid and incubated at 4 °C for 1 h prior to centrifugation at  $18000 \times g$  and 4 °C for 10 min. The supernatant was further diluted with 0.1% formic acid in 50% ACN (ACN/ $\text{H}_2\text{O}$  (1:1)) containing 200 nM labetalol and diclofenac as internal standards. Standard samples were prepared the same way by spiking 5  $\mu\text{L}$  of at least eight different concentrations of the analytes into the matrix blank.

The frozen mouse brain and liver were first weighed while frozen and transferred to 2 mL of Bead Ruptor bead beating tubes prefilled with 1.4 mm ceramic beads (Omni International, Kennesaw, GA, USA). Milli-Q deionized water (Millipore, Milford, MA, USA) was added (1:4, w/v), and the samples were homogenized using Omni Bead Ruptor 24 Elite homogenizer coupled with the Omni BR Cryo cooling unit. Samples handling and homogenization were conducted at a cold temperature ( $\approx 4$  °C). A total of 50  $\mu\text{L}$  of tissue homogenates was then mixed carefully with 150  $\mu\text{L}$  of 0.1% formic acid in ACN and centrifuged at

$18000 \times g$  for 10 min at 4 °C. The supernatants were further diluted with 50% ACN containing labetalol and diclofenac. Standard samples were prepared the exact same way by spiking 5  $\mu\text{L}$  of at least eight different concentrations of the analytes into the matrix blank.

**4.10.2. LC–MS/MS Quantification of the Studied Compounds.** The studied compounds were separated using a reversed-phase column (Zobrax SB-C18, 50 mm  $\times$  2.1 mm, 1.8  $\mu\text{m}$ ; Agilent Technologies, Santa Clara, CA, USA) and LC eluents of 0.1% formic acid in water (A) and acetonitrile (B) for the prodrugs and SA and using 35% methanol in water (A) and methanol (B) for FLB, NAP, and IBU. Labetalol and diclofenac were used as internal standards for the prodrugs and parent drugs, respectively. The injection volume was 5  $\mu\text{L}$  for all the samples, and the column temperature was 40 °C for all the prodrugs and SA samples and 60 °C for FLB, NAP, and IBU samples. The prodrugs and SA were then eluted following a constant flow rate of 0.3 mL/min and a gradient of 5% B for 2 min, followed by 5–95% B for 8 min before re-equilibrating the column again for 3 min. FLB and NAP were eluted following a constant flow rate of 0.3 mL/min and a gradient of 60% B for 1.5 min, followed by 60–95% B for 1.5 min and 95% B of the column washing phase for 3 min before re-equilibrating the column again for 3 min. IBU was eluted, however, using a different constant flow rate of 0.4 mL/min and a gradient of 15% B for 1 min, followed by 15–90% B for 8 min and 90% B of column washing phase for 3 min before re-equilibrating the column again for 3 min. The prodrugs and labetalol were analyzed using a UPLC system coupled with a triple quadrupole mass spectrometer with an electrospray ionization source in the positive mode (UPLC 1290 and MSD 6410, Agilent Technologies, Santa Clara, CA, USA) following the transitions listed in [Table 5](#). Salicylic acid and

**Table 5. Ionization Parameters of the Studied Compounds Required for the LC–MS/MS Methods**

compound	precursor ion	product ion	fragmentor voltage (V)	collision energy (V)	polarity
flurbiprofen	243	199	380	10	negative
prodrug 1	407	361	170	13	positive
naproxen	229	170	380	10	negative
prodrug 4	393	347, 185	150	15	positive
ibuprofen	205	161	380	5	negative
prodrug 3	369	323, 161	140	13	positive
salicylic acid	137	93	100	13	negative
prodrug 2	301	255, 181	100	11	positive
diclofenac <sup>a</sup>	294	250	50	3	negative
labetalol <sup>a</sup>	329	294, 162	70	10	positive

<sup>a</sup>Internal standards.

diclofenac, however, were analyzed in the negative ionization mode. On the other hand, FLB, NAP, and IBU were analyzed using a triple quadrupole instrument with iFunnel technology and an electrospray ionization source in the negative mode (UPLC 1290 and MSD 6495, Agilent Technologies, Santa Clara, CA, USA) following the transitions listed in [Table 5](#). The method optimizations and instrumentation are explained further in appendix 1 in the [Supplementary Information](#).

**4.10.3. Method Validation.** The LC–MS methods were validated according to the U.S. Food and Drug Administration guidance for method validation.<sup>49</sup> The validation parameters of the assays were followed such as calibration, quality control, selectivity, sensitivity, accuracy, precision, recovery, stability, and dilution effects ([Supplementary Information](#), Appendix 1). The lower limits of quantifications of FLB, IBU, and NAP, were 0.77, 0.65, and 0.72 ng/mL, respectively, which is, to our knowledge, the most sensitive, easy, and quick LC–MS method for their quantifications in biological samples.

**4.11. Pharmacokinetics Modeling, Calculations, and Statistical Analysis.** The unbound fractions of the studied compounds in homogenates ( $f_{u, \text{homogenate}}$ ) were calculated by equilibrium dialysis following the instructions from the manufacturer (Thermo Scientific, Single-Use RED Plates) and the formula

$$(f_{u,\text{homogenate}}) = \frac{\text{Concentration in buffer chamber}}{\text{Concentration in reaction chamber}} \times 100\%$$

The effect of tissue dilution of the homogenates ( $D$ ) was compensated to calculate the unbound tissue fraction ( $f_{u,\text{tissue}}$ ) as described by Kalvass et al.<sup>43</sup> using the following formula:

$$(f_{u,\text{tissue}}) = \frac{f_{u,\text{homogenate}}}{D - (D - 1) \times f_{u,\text{homogenate}}} \times 100\%$$

The brain, liver, and plasma drug concentrations were analyzed using an add-in program in Microsoft Excel (PKSolver).<sup>50</sup> After we followed the noncompartmental analysis mode, several PK parameters were generated. The area under the curve (AUC) was calculated based on the linear trapezoidal method, while the terminal elimination slope was calculated based on at least the last three data points. Other PK parameters were also obtained, such as  $T_{\text{max}}$ ,  $C_{\text{max}}$ , half-life ( $t_{1/2}$ ), and the apparent volume of distribution ( $V_{z/f}$ ).

The brain uptake partition coefficient parameters were calculated as described by Hammarlund-Udenaes et al.<sup>51</sup> The values of  $K_{p,\text{brain}}$  and  $K_{p,u,\text{brain}}$  were calculated from the following formulas:

$$K_{p,\text{brain}} = \frac{\text{AUC}_{\text{brain,total}}}{\text{AUC}_{\text{plasma,total}}}$$

$$K_{p,u,\text{brain}} = \frac{\text{AUC}_{\text{brain,total}}}{\text{AUC}_{\text{plasma,unbound}}}$$

Whereas the  $\text{AUC}_{\text{tissue,unbound}}$  values were calculated from the formula

$$\text{AUC}_{\text{tissue,unbound}} = \text{AUC}_{\text{tissue,total}} \times f_{u,\text{tissue}}$$

The cellular kinetic parameters ( $V_{\text{max}}$ ,  $K_m$ , and  $\text{IC}_{50}$ ) were obtained by performing nonlinear regression analysis. The statistical difference between groups were tested by performing one-way ANOVA followed by Bonferroni's multiple comparison test using GraphPad Prism 5, while probability values of  $<0.05$  are considered statistically significant.

## 5. CONCLUSION

The transporter-mediated brain delivery via LAT1 utilization is a promising approach to deliver small-sized drugs not only across the blood–brain barrier but also into the brain parenchymal cells (astrocytes and microglia). Because cyclooxygenases are located intracellularly, delivering the anti-inflammatory drugs into the activated astrocytes and microglia can better help with alleviating the neuroinflammation. This can be achieved by developing LAT1-utilizing prodrugs that can release the active parent drugs specifically into the target sites. Furthermore, in the present study, we identified a functional LAT1 transporter in the human immortalized microglia. Hence, this approach can be further translated into a human approach. As an example, we showed the improved localization of the LAT1-utilizing prodrugs into the mouse and human brain parenchymal cells. Additionally, the LAT1-utilizing prodrugs showed promising pharmacokinetics in mice. The salicylic acid prodrug was able to cross the BBB at a rate 5 times higher than that of salicylic acid itself, and it releases its parent drug specifically in the mouse brain. This targeted delivery achieved both enhanced localization into brain cells and minimal peripheral exposure.

The other structurally similar LAT1-utilizing prodrugs of flurbiprofen, ibuprofen, and naproxen also showed improved localization into the mouse and human brain parenchymal cells. However, their pharmacokinetics in mice were affected by other factors such as molecular weight, protein binding, and bioconversion. The flurbiprofen prodrug was not able to release its parent drug in any tissue due to the high plasma and liver protein binding. The ibuprofen prodrug released its parent drug

slowly in the mouse plasma, and thus, it did not improve the brain delivery of its parent drug. Lastly, the naproxen prodrug was transported and released its parent drug into the mouse brain. Although the released amount of naproxen from its LAT1-utilizing prodrug was lower than what was achieved from naproxen itself, the naproxen prodrug released the naproxen specifically in the mouse brain. Hence, minimal peripheral exposure and less adverse effects can be achieved. Therefore, when designing LAT1-utilizing brain-targeted prodrugs, the properties of the whole compound, including molecular weight, lipophilicity, and nonspecific binding, should be considered.

## ■ ASSOCIATED CONTENT

### Supporting Information

The Supporting Information is available free of charge at <https://pubs.acs.org/doi/10.1021/acscchemneuro.0c00564>.

Correlation between the lipophilicity and unbound fractions of the studied compounds in the mouse tissues; stability of the studied compounds; cellular uptake of the studied compounds in mouse primary astrocytes, BV2, and SV40 cells; LC–MS–SRM/MRM transitions of absolute protein quantification for the membrane transporters and examples of the signal peaks; and validation of the quantitative LC–MS/MS methods for the studied compounds (PDF)

## ■ AUTHOR INFORMATION

### Corresponding Author

Ahmed B. Montaser – School of Pharmacy, Faculty of Health Sciences, University of Eastern Finland, FI-70211 Kuopio, Finland; [orcid.org/0000-0003-4511-467X](https://orcid.org/0000-0003-4511-467X); Phone: +358417537797; Email: [ahmed.montaser@uef.fi](mailto:ahmed.montaser@uef.fi)

### Authors

Julia Järvinen – School of Pharmacy, Faculty of Health Sciences, University of Eastern Finland, FI-70211 Kuopio, Finland

Susanne Löffler – School of Pharmacy, Faculty of Health Sciences, University of Eastern Finland, FI-70211 Kuopio, Finland

Johanna Huttunen – School of Pharmacy, Faculty of Health Sciences, University of Eastern Finland, FI-70211 Kuopio, Finland

Seppo Auriola – School of Pharmacy, Faculty of Health Sciences, University of Eastern Finland, FI-70211 Kuopio, Finland

Marko Lehtonen – School of Pharmacy, Faculty of Health Sciences, University of Eastern Finland, FI-70211 Kuopio, Finland

Aaro Jalkanen – School of Pharmacy, Faculty of Health Sciences, University of Eastern Finland, FI-70211 Kuopio, Finland

Kristiina M. Huttunen – School of Pharmacy, Faculty of Health Sciences, University of Eastern Finland, FI-70211 Kuopio, Finland; [orcid.org/0000-0002-1175-8517](https://orcid.org/0000-0002-1175-8517)

Complete contact information is available at:

<https://pubs.acs.org/10.1021/acscchemneuro.0c00564>

### Author Contributions

The manuscript was written through the contributions of all authors. A.B.M., M.L., A.J., and K.M.H. participated in research design. A.B.M., J.J., S.L., J.H., and A.J. conducted experiments.

A.B.M., S.A., M.L., A.J., and K.M.H. contributed to new reagents or analytical tools. A.B.M. wrote the manuscript. S.A., M.L., A.J. and K.M.H. revised the manuscript. All authors have given approval to the final version of the manuscript.

### Funding

The study was financially supported by the Academy of Finland [grant numbers 294227, 294229, 307057, 311939], Sigrid Juselius Foundation [2015–2020], and the doctoral program of the University of Eastern Finland.

### Notes

The authors declare no competing financial interest.

## ACKNOWLEDGMENTS

The authors would like to thank Prof. Mikko Hiltunen for providing the BV2 cells, Prof. Tarja Malm for providing the SV40 cells, Dr. Kati-Sisko Vellonen for providing the primary astrocytes, Mrs. Tiina Koivunen for the technical assistance with prodrug syntheses and nonspecific protein-binding studies, Mrs. Sari Ukkonen for the technical assistance with the cellular uptake studies, and Ms. Agathe Hügele for performing the stability studies in the cellular homogenates. The Mass Spectrometry Laboratory is supported by Biocentre Finland and Biocentre of Kuopio.

## ABBREVIATIONS

LAT1	L-type amino acid transporter 1
BBB	blood–brain barrier
LC-MS	liquid chromatography–tandem mass spectrometry
UPLC	ultra performance liquid chromatography
SRM/MRM	selected reaction monitoring/multiple reaction monitoring
ACN	acetonitrile
DMSO	dimethyl sulfoxide

## REFERENCES

- (1) Lodish, H. F., Berk, A., Kaiser, C., Krieger, M., Bretscher, A., Ploegh, H. L., Amon, A., and Martin, K. C. (2016) Transmembrane Transport of Ions and small Molecules. In *Molecular Cell Biology*, pp 474–510, W.H. Freeman-Macmillan Learning, New York.
- (2) Enerson, B. E., and Drewes, L. R. (2006) The Rat Blood–Brain Barrier Transcriptome. *J. Cereb. Blood Flow Metab.* 26, 959–973.
- (3) Cesar-Razquin, A., Snijder, B., Frappier-Brinton, T., Isserlin, R., Gyimesi, G., Bai, X., Reithmeier, R. A., Hepworth, D., Hediger, M. A., Edwards, A. M., and Superti-Furga, G. (2015) A Call for Systematic Research on Solute Carriers. *Cell* 162, 478–487.
- (4) De Vruhe, R. L. A., Smith, P. L., and Lee, C. P. (1998) Transport of L-Valine-Acyclovir via the Oligopeptide Transporter in the Human Intestinal Cell Line, Caco-2. *J. Pharmacol. Exp. Ther.* 286, 1166–1170.
- (5) Ganapathy, M. E., Huang, W., Wang, H., Ganapathy, V., and Leibach, F. H. (1998) Valacyclovir: A substrate for the intestinal and renal peptide transporters PEPT1 and PEPT2. *Biochem. Biophys. Res. Commun.* 246, 470–475.
- (6) Vale, N. (2016) Amino Acids and Peptides in Medicine: Old or New Drugs?. In *Biomedical Chemistry: Current Trends and Developments*, pp 193, De Gruyter.
- (7) Takahashi, Y., Nishimura, T., Higuchi, K., Noguchi, S., Tega, Y., Kurosawa, T., Deguchi, Y., and Tomi, M. (2018) Transport of Pregabalin Via L-Type Amino Acid Transporter 1 (SLC7A5) in Human Brain Capillary Endothelial Cell Line. *Pharm. Res.* 35, 246.
- (8) Smith, Q. R. (2005) Carrier-mediated transport to enhance drug delivery to brain. *Int. Congr. Ser.* 1277, 63–74.
- (9) Wang, B., Hu, L., and Siahaan, T. J. (2016) Pathways for drug delivery to the central nervous system. In *Drug Delivery: Principles and Applications*, 2nd ed., pp 360–370, John Wiley & Sons, Inc..
- (10) Duelli, R., Enerson, B. E., Gerhart, D. Z., and Drewes, L. R. (2000) Expression of large amino acid transporter LAT1 in rat brain endothelium. *J. Cereb. Blood Flow Metab.* 20, 1557–1562.
- (11) Scalise, M., Galluccio, M., Console, L., Pochini, L., and Indiveri, C. (2018) The Human SLC7A5 (LAT1): The Intriguing Histidine/Large Neutral Amino Acid Transporter and Its Relevance to Human Health. *Front. Chem.* 6, 243.
- (12) Huttunen, J., Peltokangas, S., Gynther, M., Natunen, T., Hiltunen, M., Auriola, S., Ruponen, M., Vellonen, K., and Huttunen, K. M. (2019) L-Type Amino Acid Transporter 1 (LAT1/Lat1)-Utilizing Prodrugs Can Improve the Delivery of Drugs into Neurons, Astrocytes and Microglia. *Sci. Rep.* 9, 12860.
- (13) Puris, E., Gynther, M., de Lange, E. C.M., Auriola, S., Hammarlund-Udenaes, M., Huttunen, K. M., and Loryan, I. (2019) Mechanistic Study on the Use of the L-Type Amino Acid Transporter 1 for Brain Intracellular Delivery of Ketoprofen via Prodrug: A Novel Approach Supporting the Development of Prodrugs for Intracellular Targets. *Mol. Pharmaceutics* 16, 3261–3274.
- (14) Markowicz-Piasecka, M., Huttunen, J., Montaser, A., and Huttunen, K. M. (2020) Hemocompatible LAT1-inhibitor can induce apoptosis in cancer cells without affecting brain amino acid homeostasis. *Apoptosis* 25, 426–440.
- (15) Gynther, M., Puris, E., Peltokangas, S., Auriola, S., Kanninen, K. M., Koistinaho, J., Huttunen, K. M., Ruponen, M., and Vellonen, K. (2019) Alzheimer's Disease Phenotype or Inflammatory Insult Does Not Alter Function of L-Type Amino Acid Transporter 1 in Mouse Blood-Brain Barrier and Primary Astrocytes. *Pharm. Res.* 36, 17.
- (16) Kanai, Y., Segawa, H., Miyamoto, K., Uchino, H., Takeda, E., and Endou, H. (1998) Expression cloning and characterization of a transporter for large neutral amino acids activated by the heavy chain of 4F2 antigen (CD98). *J. Biol. Chem.* 273, 23629–23632.
- (17) Uchino, H., Kanai, Y., Kim, D. K., Wempe, M. F., Chairoungdua, A., Morimoto, E., Anders, M. W., and Endou, H. (2002) Transport of amino acid-related compounds mediated by L-type amino acid transporter 1 (LAT1): insights into the mechanisms of substrate recognition. *Mol. Pharmacol.* 61, 729–737.
- (18) Geier, E. G., Schlessinger, A., Fan, H., Gable, J. E., Irwin, J. J., Sali, A., and Giacomini, K. M. (2013) Structure-based ligand discovery for the Large-neutral Amino Acid Transporter 1, LAT-1. *Proc. Natl. Acad. Sci. U. S. A.* 110, 5480–5485.
- (19) Ylikangas, H., Malmioja, K., Peura, L., Gynther, M., Nwachukwu, E. O., Leppanen, J., Laine, K., Rautio, J., Lahtela-Kakkonen, M., Huttunen, K. M., and Poso, A. (2014) Quantitative insight into the design of compounds recognized by the L-type amino acid transporter 1 (LAT1). *ChemMedChem* 9, 2699–2707.
- (20) Puris, E., Gynther, M., Huttunen, J., Petsalo, A., and Huttunen, K. M. (2017) L-type amino acid transporter 1 utilizing prodrugs: How to achieve effective brain delivery and low systemic exposure of drugs. *J. Controlled Release* 261, 93–104.
- (21) Peura, L., Malmioja, K., Laine, K., Leppanen, J., Gynther, M., Isotalo, A., and Rautio, J. (2011) Large amino acid transporter 1 (LAT1) prodrugs of valproic acid: new prodrug design ideas for central nervous system delivery. *Mol. Pharmaceutics* 8, 1857–1866.
- (22) Peura, L., Malmioja, K., Huttunen, K., Leppänen, J., Hämäläinen, M., Forsberg, M. M., Rautio, J., and Laine, K. (2013) Design, Synthesis and Brain Uptake of LAT1-Targeted Amino Acid Prodrugs of Dopamine. *Pharm. Res.* 30, 2523–2537.
- (23) Puris, E., Gynther, M., Huttunen, J., Auriola, S., and Huttunen, K. M. (2019) L-type amino acid transporter 1 utilizing prodrugs of ferulic acid revealed structural features supporting the design of prodrugs for brain delivery. *Eur. J. Pharm. Sci.* 129, 99–109.
- (24) Huttunen, K. M., Gynther, M., Huttunen, J., Puris, E., Spicer, J. A., and Denny, W. A. (2016) A Selective and Slowly Reversible Inhibitor of L-Type Amino Acid Transporter 1 (LAT1) Potentiates Antiproliferative Drug Efficacy in Cancer Cells. *J. Med. Chem.* 59, 5740–5751.
- (25) Gynther, M., Laine, K., Ropponen, J., Leppänen, J., Mannila, A., Nevalainen, T., Savolainen, J., Järvinen, T., and Rautio, J. (2008) Large

Neutral Amino Acid Transporter Enables Brain Drug Delivery via Prodrugs. *J. Med. Chem.* 51, 932–936.

(26) Guzman-Martinez, L., Maccioni, R. B., Andrade, V., Navarrete, L. P., Pastor, M. G., and Ramos-Escobar, N. (2019) Neuroinflammation as a Common Feature of Neurodegenerative Disorders. *Front. Pharmacol.* 10, 1008.

(27) Liddelow, S. A., and Barres, B. A. (2017) Reactive Astrocytes: Production, Function, and Therapeutic Potential. *Immunity* 46, 957–967.

(28) Streit, W. J., Mrak, R. E., and Griffin, W. S. (2004) Microglia and neuroinflammation: a pathological perspective. *J. Neuroinflammation* 1, 14.

(29) Huttunen, K. M. (2018) Identification of human, rat and mouse hydrolyzing enzymes bioconverting amino acid ester prodrug of ketoprofen. *Bioorg. Chem.* 81, 494–503.

(30) Gynther, M., Peura, L., Vernerová, M., Leppänen, J., Kärkkäinen, J., Lehtonen, M., Rautio, J., and Huttunen, K. M. (2016) Amino Acid Promoiety Alters Valproic Acid Pharmacokinetics and Enables Extended Brain Exposure. *Neurochem. Res.* 41, 2797–2809.

(31) Kubo, Y., Ohtsuki, S., Uchida, Y., and Terasaki, T. (2015) Quantitative Determination of Luminal and Abluminal Membrane Distributions of Transporters in Porcine Brain Capillaries by Plasma Membrane Fractionation and Quantitative Targeted Proteomics. *J. Pharm. Sci.* 104, 3060–3068.

(32) Ozben, T., and Ozben, S. (2019) Neuro-inflammation and anti-inflammatory treatment options for Alzheimer's disease. *Clin. Biochem.* 72, 87–89.

(33) T. Heneka, M., P. Kummer, M., Weggen, S., Bulic, B., Multhaup, G., Muntter, L., Hull, M., Pflanzner, T., and U. Pietrzik, C. (2011) Molecular mechanisms and therapeutic application of NSAIDs and derived compounds in Alzheimer's disease. *Curr. Alzheimer Res.* 8, 115–131.

(34) Lleo, A., Galea, E., and Sastre, M. (2007) Molecular targets of non-steroidal anti-inflammatory drugs in neurodegenerative diseases. *Cell. Mol. Life Sci.* 64, 1403–1418.

(35) Nguyen, H. M., di Lucente, J., Chen, Y., Cui, Y., Ibrahim, R. H., Pennington, M. W., Jin, L., Maezawa, I., and Wulff, H. (2020) Biophysical basis for Kv1.3 regulation of membrane potential changes induced by P2 × 4-mediated calcium entry in microglia. *Glia* 68, 2377–2394.

(36) Rautio, J., Laine, K., Gynther, M., and Savolainen, J. (2008) Prodrug approaches for CNS delivery. *AAPS J.* 10, 92–102.

(37) Parepally, J. M., Mandula, H., and Smith, Q. R. (2006) Brain uptake of nonsteroidal anti-inflammatory drugs: ibuprofen, flurbiprofen, and indomethacin. *Pharm. Res.* 23, 873–881.

(38) Kamble, S., Loadman, P., Abraham, M. H., and Liu, X. (2018) Structural properties governing drug-plasma protein binding determined by high-performance liquid chromatography method. *J. Pharm. Biomed. Anal.* 149, 16–21.

(39) Uchida, Y., Ohtsuki, S., Katsukura, Y., Ikeda, C., Suzuki, T., Kamiie, J., and Terasaki, T. (2011) Quantitative targeted absolute proteomics of human blood–brain barrier transporters and receptors. *J. Neurochem.* 117, 333–345.

(40) Stefan, S. M., and Wiese, M. (2019) Small-molecule inhibitors of multidrug resistance-associated protein 1 and related processes: A historic approach and recent advances. *Med. Res. Rev.* 39, 176–264.

(41) Chandrasekharan, N. V., and Simmons, D. L. (2004) The cyclooxygenases. *Genome Biol.* 5, 241.

(42) Rautio, J., Kumpulainen, H., Heimbach, T., Oliyai, R., Oh, D., Järvinen, T., and Savolainen, J. (2008) Prodrugs: design and clinical applications. *Nat. Rev. Drug Discovery* 7, 255–270.

(43) Kalvass, J. C., and Maurer, T. S. (2002) Influence of nonspecific brain and plasma binding on CNS exposure: implications for rational drug discovery. *Biopharm. Drug Dispos.* 23, 327–338.

(44) Pihlaja, R., Koistinaho, J., Malm, T., Sikkilä, H., Vainio, S., and Koistinaho, M. (2008) Transplanted astrocytes internalize deposited beta-amyloid peptides in a transgenic mouse model of Alzheimer's disease. *Glia* 56, 154–163.

(45) Jankowsky, J. L., Fadale, D. J., Anderson, J., Xu, G. M., Gonzales, V., Jenkins, N. A., Copeland, N. G., Lee, M. K., Younkin, L. H., Wagner, S. L., Younkin, S. G., and Borchelt, D. R. (2004) Mutant presenilins specifically elevate the levels of the 42 residue beta-amyloid peptide in vivo: evidence for augmentation of a 42-specific gamma secretase. *Hum. Mol. Genet.* 13, 159–170.

(46) Janabi, N., Peudenié, S., Héron, B., Ng, K. H., and Tardieu, M. (1995) Establishment of human microglial cell lines after transfection of primary cultures of embryonic microglial cells with the SV40 large T antigen. *Neurosci. Lett.* 195, 105–108.

(47) Uchida, Y., Tachikawa, M., Obuchi, W., Hoshi, Y., Tomioka, Y., Ohtsuki, S., and Terasaki, T. (2013) A study protocol for quantitative targeted absolute proteomics (QTAP) by LC-MS/MS: application for inter-strain differences in protein expression levels of transporters, receptors, claudin-5, and marker proteins at the blood–brain barrier in ddY, FVB, and C57BL/6J mice. *Fluids Barriers CNS* 10, 21.

(48) Gynther, M., Proietti Silvestri, I., Hansen, J. C., Hansen, K. B., Malm, T., Ishchenko, Y., Larsen, Y., Han, L., Kayser, S., Auriola, S., Petsalo, A., Nielsen, B., Pickering, D. S., and Bunch, L. (2017) Augmentation of Anticancer Drug Efficacy in Murine Hepatocellular Carcinoma Cells by a Peripherally Acting Competitive N-Methyl-D-aspartate (NMDA) Receptor Antagonist. *J. Med. Chem.* 60, 9885–9904.

(49) U.S. Food and Drug Administration (2018) *Bioanalytical Method Validation Guidance for Industry*, <https://www.fda.gov/downloads/drugs/guidances/ucm070107.pdf> (accessed July 2019).

(50) Zhang, Y., Huo, M., Zhou, J., and Xie, S. (2010) PKSolver: An add-in program for pharmacokinetic and pharmacodynamic data analysis in Microsoft Excel. *Comp. Meth. Prog. Bio.* 99, 306–314.

(51) Hammarlund-Udenaes, M., Friden, M., Syvanen, S., and Gupta, A. (2008) On the rate and extent of drug delivery to the brain. *Pharm. Res.* 25, 1737–1750.